CONTRACT REPORT

FINAL REPORT

StormTech Arch Evaluation

Project No: 003239

by Dr Hanson Ngo and Dr Neal Lake

for Cubic Solutions Pty Ltd

StormTech Arch Evaluation

for Cubic Solutions Pty Ltd

	Reviewed
Project Leader	
	Neal Lake
Quality Manager	
	Rudolph Kotze

003239
March 2012

ARRB Group Ltd
ABN 68 004 620 651

Victoria
500 Burwood Highway
Vermont South VIC 3133
Australia
P: +61 3 9881 1555
F: +61 3 9887 8104
info@arrb.com.au

Western Australia
191 Carr Place
Leederville WA 6007
Australia
P: +61 8 9227 3000
F: +61 8 9227 3030
arrb.wa@arrb.com.au

New South Wales
2-14 Mountain St
Ultimo NSW 2007
Australia
P: +61 2 9282 4444
F: +61 2 9280 4430
arrb.nsw@arrb.com.au

Queensland
123 Sandgate Road
Albion QLD 4010
Australia
P: +61 7 3260 3500
F: +61 7 3862 4699
arrb.qld@arrb.com.au

South Australia
Level 5, City Central,
Suite 507, 147 Pirie Street
Adelaide SA 5000
Australia
P: +61 8 7200 2659
F: +61 8 8223 7406
arrb.sa@arrb.com.au

Luxmoore Parking Consulting
Ground Floor
12 Wellington Parade
East Melbourne, VIC 3002
P: +61 3 9417 5277
F: +61 3 9416 2602

International offices:
Dubai, United Arab Emirates
Xiamen, People's Republic of China

SUMMARY

CubicSolutions requested ARRB to carry out an evaluation of the DC-780 StormTech stormwater chamber in accordance with the relevant Australian standards.

The content of the report includes

1. structural evaluation of the traffic load carrying capacity of the DC-780 StormTech stormwater polypropylene chamber using the relevant Australian Standards;
2. calculation of minimum and maximum cover depths that are in compliance with the AS 5100 road loadings; and
3. sensitivity analyses of the results to varying the 50 year modulus of the chamber material.

Various structural models were analysed using the public domain finite element computer program CANDE. The chamber geometry was provided by Cubic Solutions and was verified on an actual segment of DC-780. Material properties of the polypropylene were based on test results provided by Cubic Solutions.

The analyses demonstrate that the chamber capacity meets the requirements to carry the road loads in compliance with the AS 5100 standard for loading up to the M and S1600 when installed in accordance with StormTech guidelines at cover depths between 470 mm and 3660 mm. We recommend that a minimum thickness of 600 mm be used for unpaved situations to take into account the rutting over time. The thickness of foundation under the chamber foot and the minimum bearing capacity of the subgrade are also recommended to be determined by the design engineer.

CONTENTS

TABLES

FIGURES

1 INTRODUCTION

1.1 Background

CubicSolutions requested ARRB to carry out an evaluation of the DC-780 StormTech stormwater chamber in accordance with the Australian specifications, including the AS 5100 – *Bridge Design Standard*, AS/NZS 2041:1998 – *Buried Corrugated Metal Structures*, the forthcoming AS/NZS 2041.1, *Buried corrugated metal structures: part 1: design methods,* and AS/NZS 2566:1998 – *Buried Flexible Pipelines*.

The DC-780 chamber is manufactured from polypropylene (PP) by the injection molding process. The chambers are arch shaped with repeating corrugated profiles (Figure 1.1).

Figure 1.1: StormTech DC-780 chamber

The StormTech system aims at providing a cost-effective method to save land and protect water resources. This system is designed primarily to be used under parking lots thus maximising land usage for commercial and municipal applications.

Nominal specifications of DC-780 chambers are as follows:

- size: (L x W x H) 2169 x 1295 x 762 mm (85.4" x 51.0" x 30.0")
- chamber storage: 1.3 m^3 (46.2 ft^3)
- minimum installed storage: 2.2 m^3 (78.4 ft^3)
- shipping: 24 chambers/pallet, 60 end caps/pallet, and 12 pallets/truck.

Figure 1.2 presents a typical cross-section of a chamber application. The chambers are placed in rows on a compacted crushed stone foundation, with minimum clear spacing of 150 mm (6 in.) between the feet of adjacent parallel chambers, 305 mm (12 in.) clear spacing between perpendicular chambers, and surrounded by crushed stone embedment. StormTech requires crushed, angular stone below, between and 150 mm above the chambers. The majority of stone used must be between 19 mm to 50 mm in size. Subrounded and rounded stone is not acceptable (StormTech 2006).

StormTech requires a minimum of 457 mm and maximum of 3660 mm for the cover depth above the chambers. In non-paved installations where rutting from vehicles may occur, a minimum of 610 mm of cover depth is required. Those values will be used as starting points for the investigation in this report. Acceptable fill materials used for the cover layers are listed in Table 1.1.

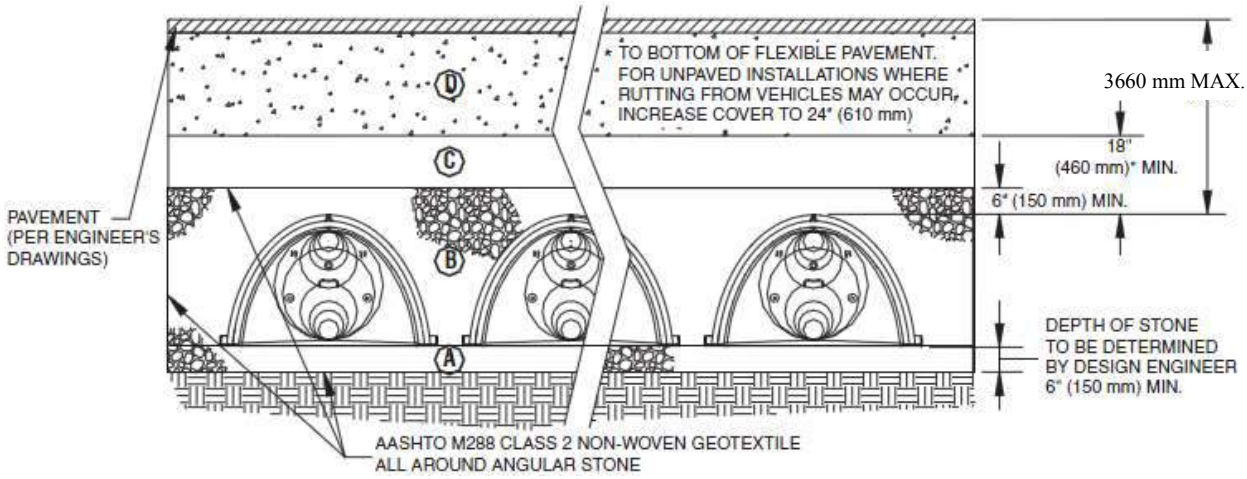

Figure 1.2: Typical installation

Table 1.1: Acceptable fill materials

Material Location	Description	AASHTO M43 Designation	AASHTO M145 Designation	Compaction/Density Requirement
(D) Fill Material from 18" (460 mm) elevation to grade above chambers	Any soil/rock materials, native soils or per engineer's plans. Check plans for pavement subgrade requirements.	N/A	N/A	Prepare per engineer's plans. Paved installations may have stringent material and preparation requirements.
(C) Fill Material for 6" (150 mm) to 18" (460 mm) elevation above chambers [24" (610 mm) for unpaved installations]	Granular well-graded soil/ aggregate mixtures, <35% fines	3, 357, 4, 467, 5, 56, 57, 6, 67, 68, 7, 78, 8, 89, 9, 10	A-1 A-2 A-3	Compact in 6" (150 mm) lifts to a min. 95% Standard Proctor density. Roller gross vehicle weight not to exceed 12,000 lbs. (53 kN). Dynamic force not to exceed 20,000 lbs. (89 kN)
(B) Embedment Stone surrounding and to a 6" (150 mm) elevation above chambers	Clean, angular stone with the majority of particles between ¾-2" (19 mm - 50 mm)	3, 357, 4, 467, 5, 56, 57	N/A	No compaction required.
(A) Foundation Stone below chambers	Clean, angular stone with the majority of particles between ¾-2" (19 mm - 50 mm)	3, 357, 4, 467, 5, 56, 57	N/A	Plate compact or roll to achieve a 95% Standard Proctor Density.

Source: StormTech 2006.

1.2 Aims

- Undertake structural evaluation of the traffic load carrying capacity of the DC-780 StormTech stormwater polypropylene chamber using Australian standards. This involves development of a finite element (FE) model using CANDE 2007. Analysis will be undertaken in accordance with ASTM F 2787-09 *Standard Practice for Structural Design of Thermoplastic Corrugated Wall Stormwater Collection Chambers*, with careful consideration of the requirements of AS 5100 – *Bridge Design Standard*, AS/NZS 2566:1998 – *Buried Flexible Pipelines* standard and AS/NZS 2041:1998 – *Buried Corrugated Metal Structures* and the new draft of this standard AS/NZS 2041.1.
- Conduct sensitivity analyses on the 50 year modulus i.e. what cover depth is required to meet AS 5100 road loads at three or four moduli. The sensitivity analysis on cover thickness will be carried out on a single chamber model.
- Determine minimum and maximum cover depths (AS 5100 compliance).

1.3 Scope

- Calculations and FE modelling are based on the DC-780 chamber only and are limited to a single configuration / set of parameters for a three chamber model at a cover of 460 mm.
- A sensitivity analysis on cover thickness is included.
- The sensitivity of the results will be investigated by varying the long-term modulus.
- The maximum depth of the chamber will be estimated.
- All relevant parameters regarding the plastic material are to be provided by Cubic Solutions. ARRB will not review or consider the accuracy of these parameters in the analysis except to ensure that relevant modulus values are consistent with the timing of load application.
- No consideration has been given to construction loads in this evaluation.

1.4 Outline

The contents of the report are briefly summarised below.

Section 2 discusses design procedures for thermoplastic material including design criteria, material characteristics and assumptions on affects of load duration on the thermoplastic chamber structure response.

Section 3 presents the structural evaluation procedure, assumptions, analysis models and finite element results for DC-780 chambers under traffic loads. Post-processing procedure and discussion of the results are also presented. A calculation for bearing capacity of foundation and subgrade soil under the chamber is included.

Section 4 outlines the results of a sensitivity analysis on cover thickness resulting in minimum and maximum values. Results of a sensitivity analysis on 50 year modulus of the chamber material are also presented.

Conclusions and recommendations are presented in Section 5.

2 THERMOPLASTIC DESIGN PROCEDURES

2.1 Design Criteria for Thermoplastic

The structural performance of buried thermoplastic structures is dependent on:

- the chamber's characteristics, i.e. wall thickness and profile, span and rise, and material
- soil stiffness of the embedment and native soil
- type and magnitude of loadings.

There are a number of codes relevant to the design of thermoplastic pipes. Within Australia there is AS/NZS 2566:1998 which is specific to the design of buried flexible pipelines and excludes arches. This code is based upon a working stress methodology where service loads are calculated (unfactored), and then compared to the material properties with a long-term factor of safety (Table 2.1 AS/NZS 2566:1998).

There are no other Australian standards which address the design of plastic structures.

In the USA there is the ASTM F2787-09 – *Standard practices for structural design of thermoplastic corrugated wall stormwater collection chambers*. This code considers both ultimate and serviceability criteria and is considered the most compatible code to use with the limit states loads of the Australian Bridge code (AS 5100.2).

The evaluation methodology used for this investigation is consistent with ASTM F2787-09.

The limit states considered in the evaluation include:

- serviceability requirements
- compression strength of the chamber to local buckling
- tensile strength of the chamber relative to the tensile strain limits
- stability of the chamber to global buckling
- capacity of the foundation material under the chamber foot
- capacity of the subgrade material to bearing from the foundation.

2.1.1 Serviceability

Deflections are limited to ensure that:

- displacements at the ground surface do not affect the road surface
- the distribution of loads assumed in the analysis are upheld
- the hydraulic function is not compromised.

Deflections are determined using the critical service loads which for AS 5100 is the W80 wheel load (unfactored) plus the dynamic load allowance for shallow installations where live loads are more critical. ASTM F2787-09 limits service deflections to 2.5% of the nominal rise or span. It is not clear in the code whether dead load is included or just live load. However, the AASHTO LRFD code (2010) clearly states that service deflections relate to live load only and this is what is assumed for this evaluation.

According to AS/NZS 2566:1998 for buried flexible pipelines, long-term deflection is assumed to be the critical deflection criteria, i.e. 50 years duration. A deflection limit of 7.5% of the pipe diameter for long-term dead load is specified. For short-term deflections, a limit of 4% is used for live load only. It is however noted that AS/NZS 2566 explicitly excludes arches.

2.1.2 Compression strength

Local buckling is assessed by determining the effective area that can carry compression loads. The effective area is determined based on the slenderness of the individual elements.

The design is then evaluated for:

- thrust only
- combined thrust and bending.

Ultimate strains are calculated using appropriate load factors from AS 5100 which are then compared to the yield strain for the thrust only case and 1.5 yield strain for the combined thrust and bending case.

As noted in the AASHTO (2010), the criterion for combined compressive strain is based on limited scope for local buckling in the web. A higher strain limit (50% higher) is allowed for the combined strain because the web elements, which experience low strains due to bending, are less likely to buckle and increase the stability of elements near the crest and valley. It is a similar concept to using plastic section capabilities in steel design where local buckling is unlikely to occur.

2.1.3 Tensile strength

The factored ultimate tensile strain is limited to the material tensile strain of the material. The factored tensile strain is calculated considering the tension due to tensile axial forces in addition to tensile forces resulting from bending.

2.1.4 Global buckling

The critical buckling thrust is determined and compared to the ultimate (factored) thrust. The critical buckling thrust is determined using the process developed by the American Water Works Association for buried plastic pipe in accordance with ASTM F2787-09.

2.1.5 Foundation strength

Bearing of the chamber foot on the foundation and bearing of the foundation on the subgrade shall be checked versus the ultimate bearing capacity. The chamber foot is idealised as a rectangular spread footing with load applied to the foundation. The load travelling from the chamber and any adjacent soil column is distributed through the foundation and applied as a spread footing to the subgrade.

2.2 Material Characteristics of Polypropylene (PP)

A long-term design basis is assumed to be the critical design consideration, as specified in both AS/NZS 2566:1998 and ASTM F2787-09.

Although most plastics show significant time-dependent stress-strain response, it is customary to treat them as elastic materials with a modulus dependent on load duration. Short-term properties are appropriate for shallow burial situations wherein live loads dominate. Long-term properties are suitable to deep burial conditions wherein design life for soil weight is in the order of 50 years (Mlynarski et al. 2008).

It is important to note however that it is generally accepted that no matter what stage of life the plastic is at the instantaneous response of the material will be as per its initial modulus properties (AASHTO 2010). The 50 year moduli do not indicate a softening of material but the time-dependent relation between stress and strain. Creep modulus is used to simulate the change in stress-strain relationships.

ASTM F2787-09 allows the theory of superposition to be used to add the long-term design actions using the long-term modulus to the short-term design actions under live load using the short-term modulus values.

According to the TRB NCHRP 619 report (Mlynarski et al. 2008), for polypropylene material, the effective Young's modulus and ultimate strength for short-term and long-term loading vary in the ranges shown in Table 2.1. The stress-strain diagram is shown in Figure 2.1 where PU is the ultimate stress and PE is the Young's modulus.

Table 2.1: Chamber material properties used in TRB NCHRP 619 report

No.	Description	MPa	ksi
1	Young's modulus for short-term loading	862-1000	125-145
2	Stress limit for short-term loading	21.37	3.1
3	Young's modulus for 50 year long-term loading	213.70	31
4	Stress limit for 50 year long-term loading	6.55-7.24	0.95-1.05

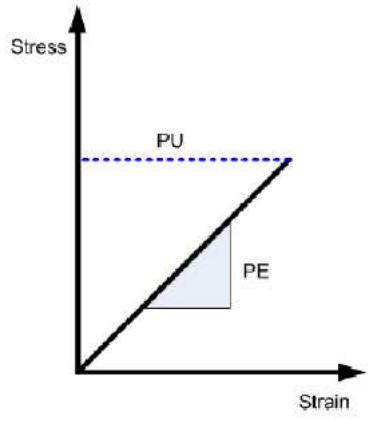

Figure 2.1: Stress-strain diagram of PP material

Source: TRB NCHRP 619 report (Mlynarski et al. 2008).

Similarly, ASTM F2418-09 S*tandard Specification for Polypropylene Corrugated Wall Stormwater Collection Chambers* requires that the minimum tensile stress at yield shall not be less than 21 MPa and the minimum flexural modulus shall not be less than 1000 MPa. It also requires that specimens fabricated in the same manner and composed of the same materials, including all additives, as the finished chambers shall have a 50-year tensile creep modulus at 23^{o}C at a stress level of 3.5 MPa not less than 165 MPa.

2.3 Load Duration

As specified in ASTM F2787-09, thermoplastic chamber structures response is dependent on load duration. For live load, chamber response must be assessed using appropriate creep moduli for two cases:

- instantaneous response (transient loads due to moving vehicle) using a short duration (1 min) creep modulus, with dynamic impact and multiple presence factors
- longer duration response (sustained loads due to parked vehicle) using a one week modulus with no dynamic impact and multiple presence factors.

For dead load, 50 year modulus values are considered.

The combined dead load and live load response is determined by superposition.

3 STRUCTURAL EVALUATION

3.1 Chamber Geometry and Placement

3.1.1 Geometry

The geometry of the chamber cross-section is taken from an AutoCAD drawing provided by Cubic Solutions and confirmed by measuring from an actual segment of DC-780 provided by Cubic Solutions (Figure 3.1). The wall profile of the chamber varies along the chamber perimeter, in which a stiffening rib is added to the corrugation crest near the base of the chamber. In addition, the thickness of the wall is also increased from 4.8 mm to 5.08 mm in the chamber leg from the foot to 480 mm above. Two cross-sections were used in the analysis, including the section at crown and the section at 240 mm above the foot.

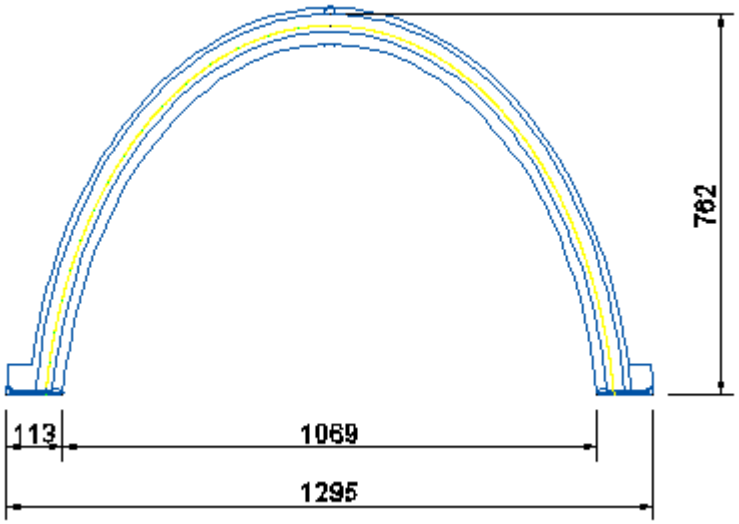

Figure 3.1: DC-780 cross-section (mm)

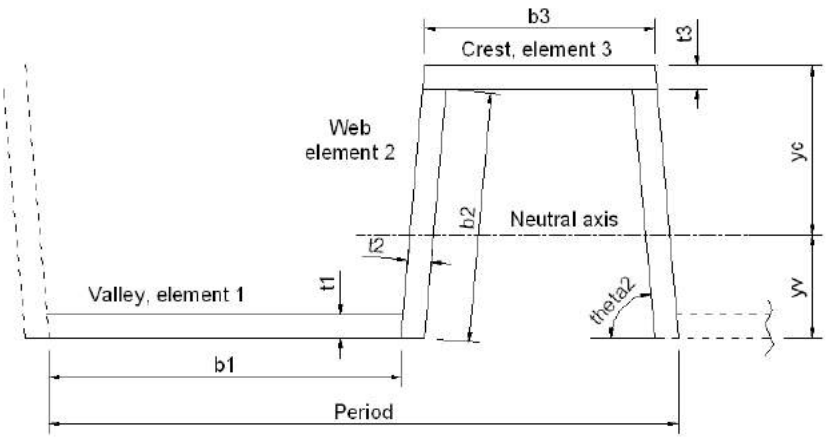

Figure 3.2: Idealised DC-780 corrugated wall cross-section at crown

The idealised cross-section of the corrugated profile at crown is shown in Figure 3.2. Detailed dimensions and sectional properties are presented in Table 3.1 and Table 3.2, respectively.

Table 3.1: Detailed dimensions of cross-section at crown

No.	Description	Denotation	Dimension (mm)	Dimension (inches)
1	Length of profile period	Period	163	6.38
2	Total height of profile section	--	70	2.76
3	Web angle with the horizontal	Theta2	81 degree	81 degree
4	Web thickness	t1, t2, t3	4.8	0.188
5	Length of valley element	b1	99	3.896
6	Length of crest element	b3	51.6	2.032
7	Length of web element	b2	65.9	2.60

Table 3.2: Idealised sectional properties of corrugated wall at crown

No.	Description	Denotation	Value	Unit
1	Unit area of idealised geometry	A_I	8.03	mm^2/mm
2	Centroidal distance from base of valley	y_v	29.14	mm
3	Centroidal distance to outside of crest	y_c	40.72	mm
4	Unit moment of inertia of idealised geometry about its centre of gravity	I_I	4837.73	mm^4/mm

The idealised cross-section and sectional properties of the corrugated profile at 240 mm above the foot is shown in Figure 3.3 and Table 3.3, respectively.

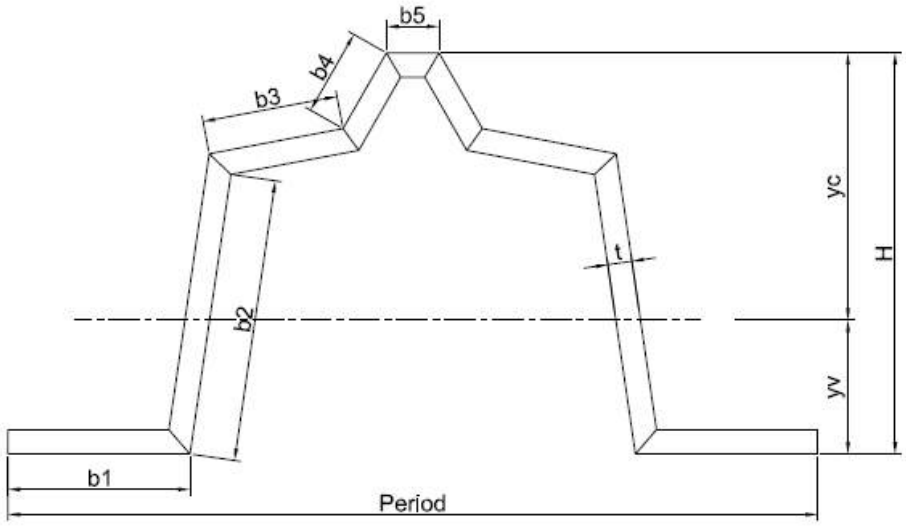

Figure 3.3: Idealised DC-780 corrugated wall cross-section at foot area

Table 3.3: Idealised sectional properties of DC-780 corrugated wall cross-section at foot area

No.	Description	Denotation	Value	Unit
1	Length of profile period	Period	168	mm
2	Total height of profile section	H	84	mm
3	Web thickness	t	5.08	mm
4	Length of valley element	b1	38.0	mm
5	Length of web element	b2	59.0	mm
6	Length of crest element	b3	28.4	mm
7	Length of crest element	b4	18.3	mm
8	Length of crest element	b5	11.0	mm
9	Unit area of idealised geometry	A_I	8.7	mm^2/mm
10	Centroidal distance from base of valley	y_v	26	mm
11	Centroidal distance to outside of crest	y_c	58	mm
12	Unit moment of inertia of idealised geometry about its centre of gravity	I_I	6804	mm^4/mm

3.1.2 Installation layout

A three chamber model is considered where the basic dimensions are shown in Table 3.4 and presented in Figure 3.4. The number of soil layers and dimensions is taken from the StormTech DC-780 cut sheet and *StormTech Design Manual* with minimum requirements as follows:

- clear spacing between chambers: 150 mm (6 in.)
- depth of fill above the crown: 460 mm (1.5 ft)
- depth of foundation layer under the chamber's foot: 230 mm (9 in.).

Note that for the current model, a minimum cover depth of 460 mm is used, thus layer D in Figure 1.2 and Table 1.1 is not present.

The sizes of the insitu soil areas underneath and at the sides of the chamber installation being taken into consideration are derived from some trial runs so that the load effects on the insitu soil beyond those areas are negligible.

Table 3.4: Detailed dimensions of DC-780 chamber layout

No.	Description	Dimension (mm)	Dimension (inches)
1	Thickness of insitusoil under the foundation	508	20.00
2	Thickness of insitusoil walls	508	20.00
3	Thickness of foundation layer	229	9.00
4	Height of embedment layer above the crown	150	6.00
5	Thickness of fill layer	310	12.00

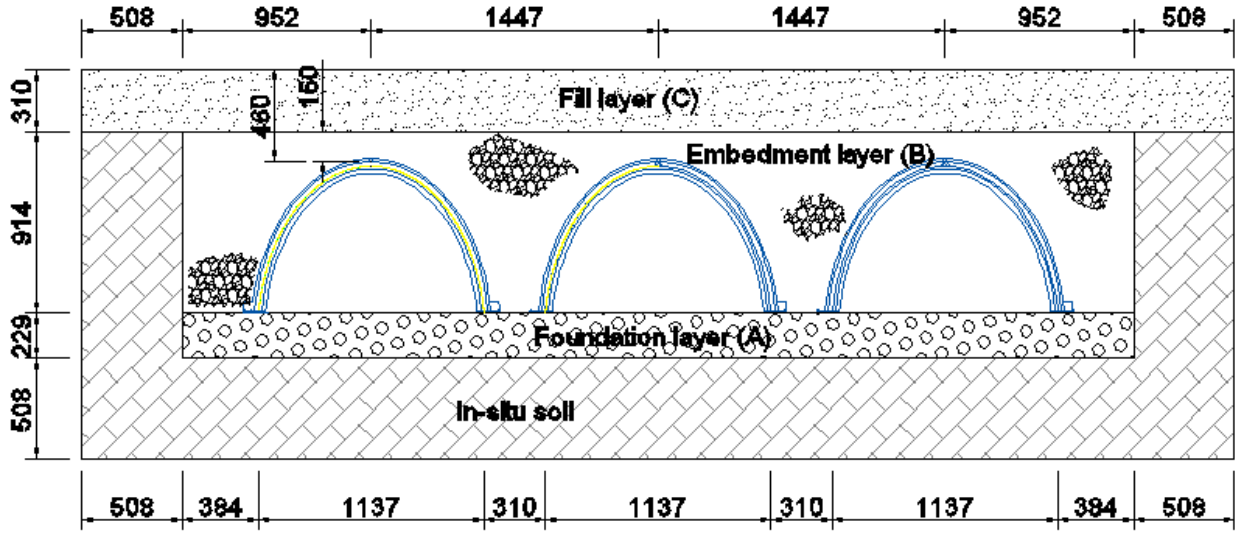

Figure 3.4: Chamber installation layout

3.1.3 Material properties

Trevor Loffel (Cubic Solutions) by email on 3 February, 2011, provided the material properties of the chambers (Table 3.5). This data is backed up by the test results shown in Figure 3.6. This set of material properties is used in this analysis.

Table 3.5: Assumed chamber material properties

No.	Description	MPa	ksi
1	Young's modulus for short-term loading	1000	145
2	Stress limit for short-term loading	21.37	3.1
3	Young's modulus for 50 year long-term loading	186	27
4	Stress limit for 50 year long-term loading	4.83	0.7
5	One week modulus	310	45
6	Poisson's ratio	0.35	0.35
7	Density of plastic material	900 kg/m^3	900 kg/m^3

These parameters are consistent with the specification of PP material in accordance with ASTM F2418-09. This specification states that the material shall have a 50 year tensile creep modulus at 23^{o}C at a stress level of 3.5 MPa not less than 165 MPa.

Figure 3.5 and Figure 3.6 were provided by Cubic Solutions and present creep modulus and strain test results, respectively, undertaken by or on behalf of StormTech by others in accordance with the ASTM F2418-09 standard. The test methods in CL6.2.6 and CL6.2.7 are used to define the slope of the logarithmic regression curves using a 10 000 hours test duration. This curve is then extrapolated to the 50 year design value.

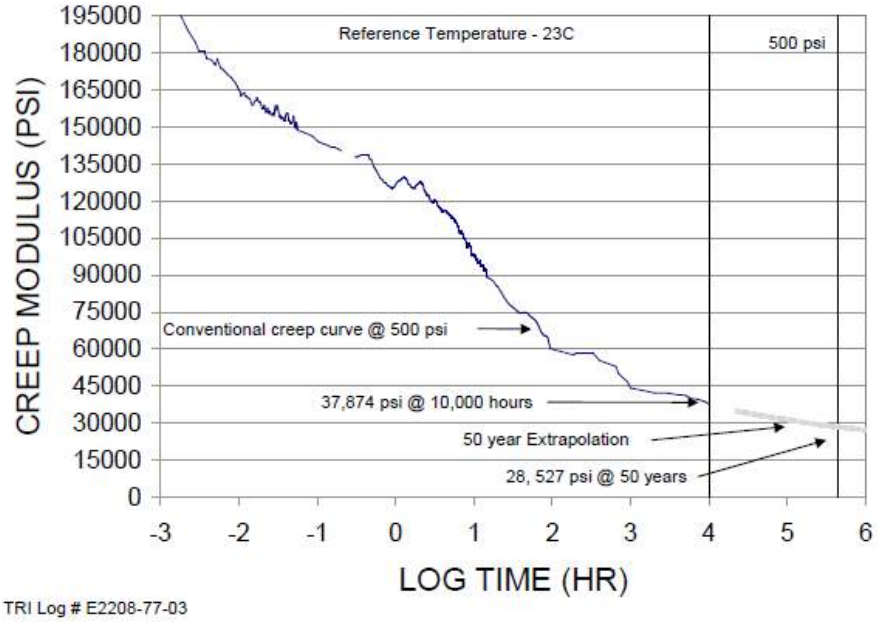

Source: Trevor Loffel, email on 11 February, 2011.

Figure 3.5: StormTech conventional creep test results for creep modulus

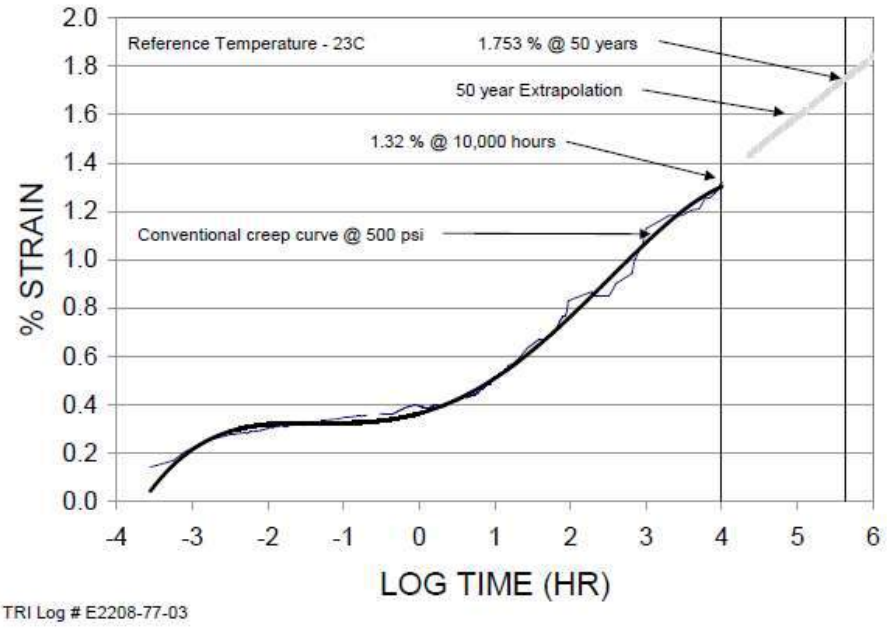

Source: Trevor Loffel, email on 11 February, 2011.

Figure 3.6: StormTech conventional creep test results for strain

The limiting compression strain should be appropriately determined from compression tests. According to ASTM F2787-09, for typical thermoplastics, the values of stiffness and strength vary with temperature, load level, and load rate. The standard reports that research, testing and analysis have shown that these same thermoplastics fail at a constant strain that is approximately

independent of load application rate or duration. The strain is a function of the resin. A value of 3.3% is used for the limiting compression strain in the current analysis (McGrath 2010).

3.1.4 Soil models

The following two soil models are selected as they are commonly used in similar applications:

- Linear elastic (isotropic): Linear elastic implies the soil stiffness remains constant irrespective of the stress state, and isotropic implies the soil stiffness is uniform in all spatial directions. This model is useful for characterising stiff insitu soils and pre-consolidated soils such as the soil remaining after excavations (Katona et al. 2008).The elastic soil model is characterised by Young's modulus and Poisson's ratio.
- Duncan and Selig models: Duncan and Duncan/Selig are variable-modulus elasticity formulations using stress-dependent equations for Young's modulus and bulk modulus. The Duncan form and Duncan/Selig form are very similar, differing slightly in the expression for the bulk modulus function. They are the two most popular (nonlinear hyperbolic) soil models extensively used for characterising the stress-dependent stiffness of backfill soil in culvert installations (Katona et al. 2008).

Table 3.6 and Table 3.7 list soil model parameters, where K = magnitude of initial tangent modulus; n = exponent for initial tangent modulus; C = cohesion intercept; Φ_0 = initial friction angle; Δ_φ = reduction of friction angle; R_f = ratio of actual failure stress to model's ultimate stress limit; K_b or B_i/P_a = magnitude of tangent bulk modulus for Duncan or Duncan/Selig, respectively; m or ε_u = bulk modulus parameter for Duncan or Duncan/Selig, respectively.

Table 3.6: Material names and values for Duncan model

MATNAM	Young's Tangent Modulus Parameters						Bulk Parameters		Density
	K	n	C	φ_0	$\Delta\varphi$	R_f	K_b	m	reference
(word)*	(--)	(--)	(psi)	(deg)	(deg)	(--)	(--)	(--)	(lb/ft^3)
CA105	600	0.40	0.0	42	9	0.7	175	0.2	150
CA95	300	0.40	0.0	36	5	0.7	75	0.2	140
CA90	200	0.40	0.0	33	3	0.7	50	0.2	135
SM100	600	0.25	0.0	36	8	0.7	450	0.0	135
SM90	300	0.25	0.0	32	4	0.7	250	0.0	125
SM85	150	0.25	0.0	30	2	0.7	150	0.0	120
SC100	400	0.60	0.5	33	0	0.7	200	0.5	135
SC90	150	0.60	0.3	33	0	0.7	75	0.5	125
SC85	100	0.60	0.2	33	0	0.7	50	0.5	120
CL100	150	0.45	0.4	30	0	0.7	140	0.2	135
CL90	90	0.45	0.2	30	0	0.7	80	0.2	125
CL85	60	0.45	0.1	30	0	0.7	50	0.2	120

*MATNAM is composed of two letters and a number defined as follows:
CA = Course Aggregates, SM = Silty Sand, SC = Silty-Clayey Sand and CL = Silty Clay
Number = percent relative compaction, per AASHTO T-99

Source: Mlynarski et al. (2008).

Table 3.7: Material names and values for Duncan/Selig model

MATNAM (word)**	Young's Tangent Modulus Parameters						Bulk Parameters***		Density reference (lb/ft^3)
	K (--)	n (--)	C (psi)	φ_0 (deg)	$\Delta\varphi$ (deg)	R_f (--)	B_i/P_a (--)	ε_u (--)	
SW100	1300	0.90	0.0	54	15	0.65	108.8	0.01	148
SW95	950	0.60	0.0	48	8.0	0.70	74.8	0.02	145
SW90	640	0.43	0.0	42	4.0	0.75	40.8	0.05	140
SW85	450	0.35	0.0	38	2.0	0.80	12.7	0.08	130
SW80	320	0.35	0.0	36	1.0	0.90	6.1	0.11	120
ML95	440	0.40	4.0	34	0.0	0.95	48.3	0.06	135
ML90	200	0.26	3.5	32	0.0	0.89	18.4	0.10	130
ML85	110	0.25	3.0	30	0.0	0.85	9.5	0.14	122
ML80	75	0.25	2.5	28	0.0	0.80	5.1	0.19	115
ML50	16	0.95	0.0	23	0.0	0.55	1.3	0.43	66
CL95	120	0.45	9.0	15	4.0	1.00	21.2	0.13	130
CL90	75	0.54	7.0	17	7.0	0.94	10.2	0.17	125
CL85	50	0.60	6.0	18	8.0	0.90	5.2	0.21	120
CL80	35	0.66	5.0	19	8.5	0.87	3.5	0.25	112

**MATNAM is composed of two letters and a number defined as follows:
SW = Gravelly Sand, ML = Sandy Silt, and CL = Silty Clay
Number = percent relative compaction, per AASHTO T-99

Source: Mlynarski et al. (2008).

Matching the descriptions of the soil layers in Table 1.1 and the above information, the following soils are selected (Table 3.8):

- The soils for the foundation layer, which are clean, crushed, angular stones with nominal size distribution 19-51 mm, compacted to 95% standard Proctor density, can be modelled by SW95 in Table 3.7.
- The soils for the embedment layer, which are clean, crushed, angular stones with nominal size distribution 19-51 mm and no compaction required, can be modelled by SW90 in Table 3.7.
- The soils for the fill layer, which are granular well-graded soil/aggregate mixture, with less than 35% fines and no compaction required, can be modelled by SW90 in Table 3.7.
- For the insitu layer, sandy soil is assumed; properties are selected based on soil properties that are compatible with the minimum allowed bearing pressure of 100 kPa. The parameters can then be selected from any geotechnical text book: density 1922 kg/m^3 (120 lb/ft^3), Young's modulus 41 MPa (6000 psi), and Poisson's ratio 0.35.

Table 3.8: Assumed soil models and types

No.	Layer	Model type	CANDE soil type
4	Fill layer C	Duncan/Selig	SW90
3	Embedment layer B	Duncan/Selig	SW90
2	Foundation layer A	Duncan/Selig	SW95
1	Insitu soil	Isotropic-Linear elastic	User: Sandy soil

3.1.5 Loading

Load cases

- Dead load: includes self-weight of all soil layers above the chamber.
- Live load: includes wheel load W80 or axle load A160 in accordance with AS 5100.
- Other cases of live load have been considered including M1600 or S1600 with 3 axles (360 kN or 240 kN) placed 1.25 m apart plus a uniform load of 6 kN/m or 24 kN/m, respectively.

Two locations of live load are also considered: wheel load at the chamber crown and wheel load at the chamber shoulder (1/4 span).

Load factor for the dead load using with uncontrolled fills is 1.50 for the ultimate limit state (ULS) and 1.20 for the serviceability limit state (SLS) (Table 5.4 AS 5100.2).

Load factor for live load

For W80 wheel load and A160 axle load, the load factors are 1.80 for ULS and 1.0 for SLS (Table 6.10A, AS 5100.2).

Accompanying lane factor

According to Table 6.6 (AS 5100.2), the maximum accompanying lane factor is 1.0 for the one-lane loaded case. For the case of two loaded lane, the factor is 1.0 for the first lane and 0.8 for the second lane. A comparison of the pressure through the earth fill of possible wheel load and axle combinations shows that the governing load case is either a single wheel load W80 for shallow installations or single-lane M1600 load for the deeper installations.

Dynamic load allowance

The dynamic load allowance for buried structures is specified in Clause 6.7.3 of AS 5100.2. For W80 wheel and M1600 loads, the dynamic load allowance is respectively 0.4 and 0.35 at the ground level, 0.1 for a depth of 2 m or more, or a linear interpolation between depths of zero and 2 m.

Distribution of wheel load through fill

The distribution of wheel load through fill is specified similarly in both AS 5100 and AS/NZS 2041 as shown in Figure 3.7. The design wheel loads are distributed through the fill, from the imprint of the rectangular wheel contact area at the road surface to a rectangular distribution area on the surface of the structure, proportioned in accordance with the wheel contact area dimensions. The resultant wheel loads are a series of concentrated loads acting on the nodes of the FE mesh (Figure 3.8).

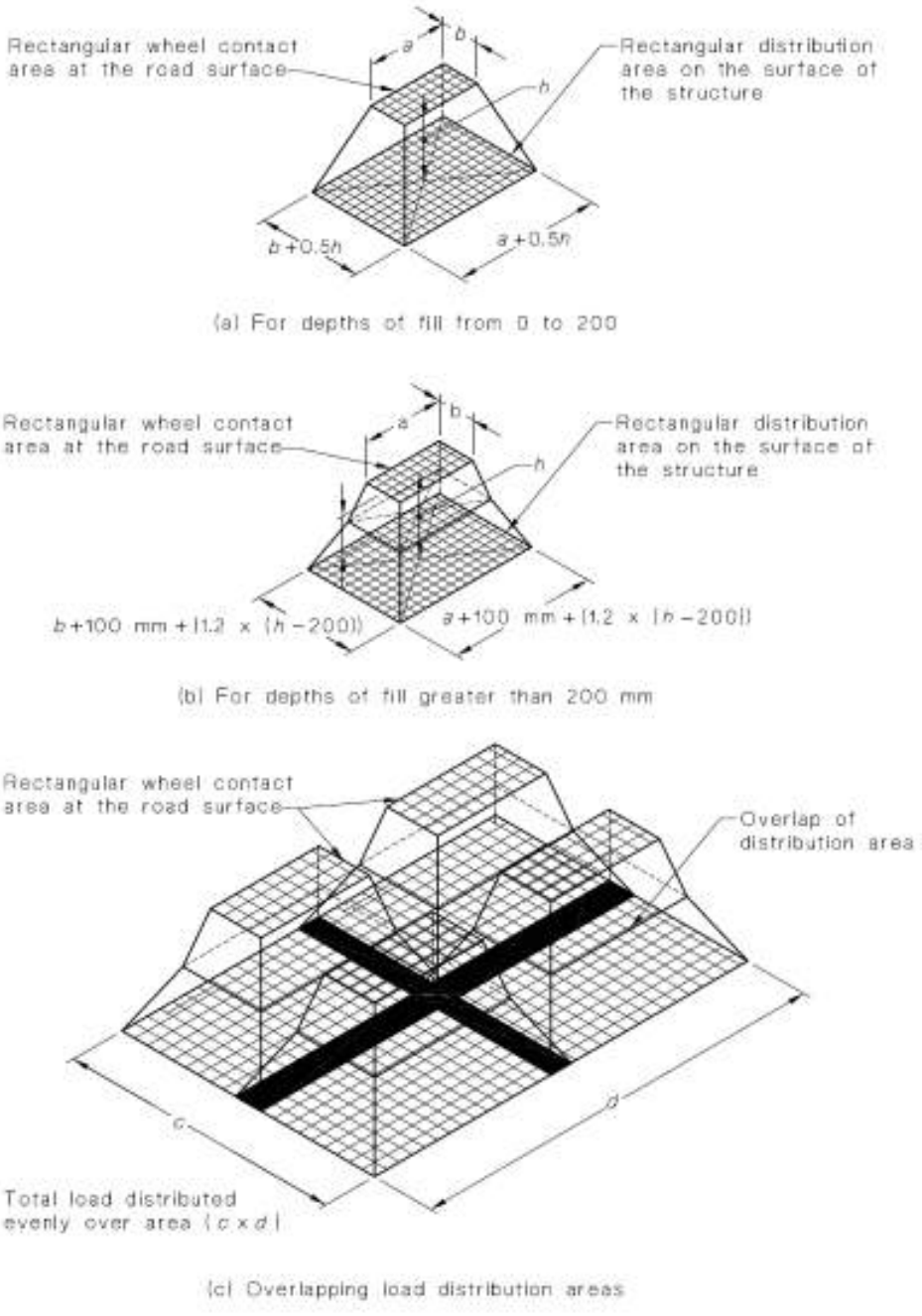

Source: draft AS/NZS 2041.1 (2010).

Figure 3.7: Distribution of wheel loads through fill

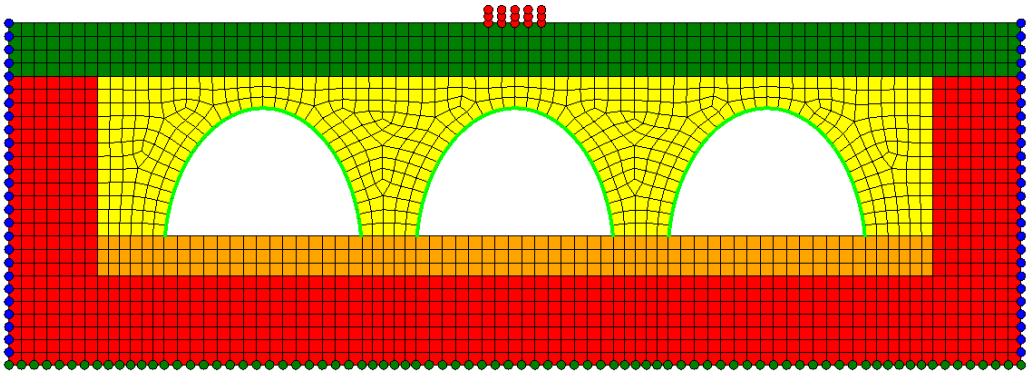

Figure 3.8: Finite element mesh

The lengths of the sides of the distribution rectangle are determined as follows:

- For depths of fill cover from 0 to 200 mm, sides of the distribution rectangle equal sides of the wheel contact rectangle + 0.5 h, where h is the depth of fill cover in millimetres.
- For depths of fill cover greater than 200 mm, sides of the distribution rectangle equal sides of wheel contact rectangles + 100 mm + 1.2 x (h − 200).

Where distribution areas from several wheel loads or axles overlap, the total load may be considered to be evenly distributed on the surface over the total area of distribution, according to AS 5100.2 clause 6.12.

The calculation procedure is described below.

For depth of fill greater than 200 mm, the out-of-plane wheel load equivalent distribution width is:

$E_{wheel} = W_{tyre} + 100mm + 1.2*(h-200mm)$.

The axle load equivalent distribution width will be:

$E_{axle} = W_{axle} + W_{tyre} + 100\ mm + 1.2*(h-200mm)$

where W_{tyre} and W_{axle} are the tyre contact width and length, respectively; h is the depth of fill.

The single wheel live load equivalent distribution (no overlap) is:

$LL_{wheel} = P_{tyre} * (1 + DLA) * ALF / E_{wheel}$,

and the axle live load equivalent distribution (overlap) is

$LL_{axle} = P_{axle} * (1 + DLA) * ALF / E_{axle}$,

where P_{tyre} and P_{axle} are tyre load and axle load, respectively, and DLA is the dynamic load allowance, and ALF is the accompanying lane factor.

The controlling load distribution LL will be the larger of the above two values LL_{wheel} and LL_{axle}.

Similar formulae are used for M1600 loads.

It is noted that LL is the load acting on a unit length on the out-of-plane direction, i.e. along the chamber's longitudinal axis. The distribution in the plane of the chamber's cross-section is not calculated through the earth fill, thus LL will be distributed on the tyre contact length (250 mm) at the surface level.

Table 3.9 presents the calculations of wheel loads distributed through fill for the depth of 460 mm.

Table 3.9: Calculation of live load through earth fills

DISTRIBUTION OF LIVE LOAD THROUGH EARTH FILL – AS 5100.2	Value	SI unit	Value	US unit
Depth of fill/cover	460	mm	1.50	ft
Design vehicle				
Axial load	160	kN	35.97	kips
Tyre load	80	kN	17.98	kips
Axle width (distance between tyres)	2000	mm	6.56	ft
Tyre contact area				
Contact width	400	mm	15.75	in
Contact length	250	mm	9.84	in
Design factors				
Accompanying lane factor	1		1	
Dynamic load allowance (for A160 and W80)	0.4		0.4	
Impact factor	1.331		1.331	
For depth of fill greater than 200 mm (AS 5100.2, clause 6.12)				
Wheel load equivalent distribution width	1174.4	mm	46.24	in
Axle load equivalent distribution width	2774.4	mm	109.23	in
Wheel live load equivalent distribution (no overlap)	0.088	kN/mm	500.08	lbf/in
Axle live load equivalent distribution (overlap)	0.074	kN/mm	423.37	lbf/in
Determine controlling distribution (wheel load)	0.088	kN/mm	500.08	lbf/in

3.2 Finite Element Analyses

3.2.1 Analysis cases

Chamber structures are checked under (i) serviceability limit state and (ii) ultimate limit state in accordance to AS 5100 and other applicable standards. In each case, three load combinations are considered, including:

- Dead load with long-term creep modulus of the chamber material (DL1).
- Live load with short-term creep modulus (2 live load locations) and dead load with long-term creep modulus (LL1 and LL2 for wheel load on crown and wheel load on shoulder, respectively).
- Live load with 1 week creep modulus (2 live load locations) and dead load with long-term creep modulus (LL3 and LL4 for wheel load on crown and wheel load on shoulder, respectively).

In addition, in order to derive analysis results for live load with short-term and one week creep moduli, another two cases were carried out: dead load with short-term creep modulus (DL2) and dead load with one week creep modulus (DL3).

Unfactored dead load and live load with accompanying lane factor and dynamic load allowance were used in the FE analysis. The load factors were included in the post-processing calculations.

3.2.2 Foot assumptions

The following assumptions are made when modelling the chamber in CANDE:

- CANDE assumes that the interface between chamber beam elements and soil elements is fully bonded. In the model, the foot of the chamber is pin-connected to the soil and it is able to move laterally with the soil. The effects of the gusset plate are not considered in this simplistic CANDE model.
- Moment will occur due to eccentricity of the foot and wall.
- Arch foot is stiffened to deal with this. If arch foot is not stiffened locally then this may affect the stability of the arch.
- The adequacy of the foot to wall connection is not considered in this evaluation. The horizontal plate of the chamber's foot was not taken into consideration in this analysis. The presence of the horizontal plate and the gusset plate connection allows the foot to spread the load in the arch walls and thus reduces high local pressure.

3.2.3 Analysis results

For each beam group, graphs can be shown for each single load step or multiple load steps for bending moment, thrust force, shear force, and displacements, etc.

Results of one analysis case are presented below for illustration, in which a model with a cover depth of 460 mm is analysed with dead load with long-term creep modulus, live load with short-term modulus, and live load with one week creep modulus. Figure 3.9 shows the locations of the beam sections on the chamber. Note that sections 40 to 60 use crown section properties and use a wall area of A_I = 8.03 mm^2 per mm (Table 3.2), while the remaining sections use foot cross-section properties and use a wall area of A_I = 8.70 mm^2 per mm (Table 3.3).

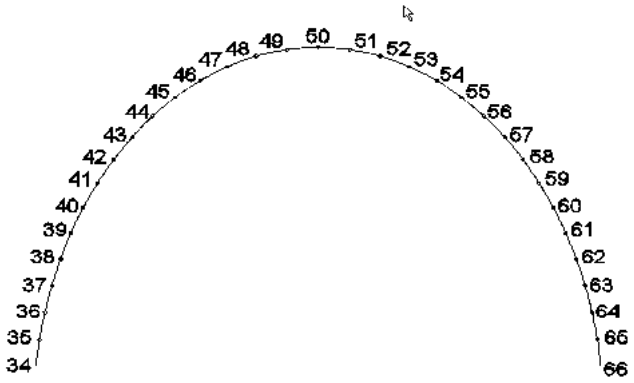

Figure 3.9: Chamber beam section locations

Table 3.10 and Table 3.11 show the analysis results of unfactored displacements and bending moments and thrust forces, respectively, of the middle chamber (chamber group 2 in Figure 3.4),

which is under the most severe loading conditions, for dead load with long-term modulus and live load (W80) with short-term modulus. Table 3.12 shows FE results for live load with one week modulus. Figure 3.11 to Figure 3.14 present several examples of the deflection shape, bending moment, thrust force and shear force, respectively, of the model. It should be noted that the deformed shapes in Figure 3.10 and Figure 3.11 are magnified to 5 times for ease of visualisation.

Table 3.10: Vertical displacements of chamber group 2 due to dead load with long-term modulus and live load with short-term modulus

Beam section no.	Long-term modulus	Short-term modulus		
	Dead load (DL1)	Dead load (DL2)	Dead load + Live load	
			Wheel load at crown (LL1)	Wheel load at shoulder (LL2)
	mm	mm	mm	mm
34	-1.206	-1.299	-7.6923	-8.5645
35	-1.403	-1.355	-7.8441	-8.766
36	-1.601	-1.417	-8.0116	-8.9968
37	-1.788	-1.479	-8.2186	-9.2783
38	-1.962	-1.539	-8.4791	-9.6191
39	-2.125	-1.597	-8.8126	-10.0484
40	-2.280	-1.653	-9.2415	-10.5948
41	-2.429	-1.710	-9.7839	-11.3188
42	-2.575	-1.767	-10.4951	-12.2404
43	-2.727	-1.826	-11.4305	-13.3645
44	-2.877	-1.886	-12.6255	-14.6627
45	-3.023	-1.944	-14.0769	-16.0498
46	-3.163	-1.997	-15.7217	-17.3774
47	-3.290	-2.044	-17.4121	-18.4412
48	-3.395	-2.079	-18.9187	-19.0262
49	-3.465	-2.102	-19.9759	-18.9741
50	-3.491	-2.110	-20.3648	-18.2515
51	-3.469	-2.103	-19.9999	-16.9738
52	-3.403	-2.082	-18.9653	-15.3649
53	-3.303	-2.049	-17.4788	-13.6777
54	-3.182	-2.005	-15.8045	-12.1168
55	-3.048	-1.955	-14.1688	-10.7989
56	-2.908	-1.900	-12.7229	-9.7587
57	-2.765	-1.843	-11.5315	-8.9634
58	-2.619	-1.787	-10.5986	-8.3469
59	-2.478	-1.732	-9.8892	-7.8439
60	-2.333	-1.677	-9.3507	-7.4269
61	-2.180	-1.621	-8.9272	-7.0911
62	-2.017	-1.564	-8.5985	-6.8357
63	-1.841	-1.503	-8.3431	-6.6439
64	-1.649	-1.440	-8.1414	-6.4961
65	-1.445	-1.377	-7.9785	-6.377
66	-1.241	-1.319	-7.8294	-6.2653

Table 3.11: Bending moments and thrust forces of chamber group 2 due to dead load with long-term modulus and live load with short-term modulus

	Long-term modulus		Short-term modulus					
	Dead load (DL1)		Dead load (DL2)		Dead load + Live load			
					Wheel load at crown (LL1)		Wheel load at shoulder (LL2)	
Beam section no.	Bending moment	Thrust force	Bending moment	Thrust force	Bending moment	Thrust force	Bending moment	Thrust force
	N-mm/mm	N/mm	N-mm/mm	N/mm	N-mm/mm	N/mm	N-mm/mm	N/mm
34	0	-4.86	0	-6.53	0	-30.07	0	-34.61
35	16.61	-4.96	33.84	-7.18	-146.03	-37.12	-156.24	-42.09
36	10.11	-4.93	30.37	-7.6	-238.68	-44.12	-258.97	-49.24
37	4.05	-4.72	18.76	-7.67	-339.07	-49.66	-352.3	-54.2
38	-1.42	-4.43	4.73	-7.51	-421.64	-52.53	-443.83	-56.45
39	-4.91	-4.1	-5.33	-7.18	-434.42	-53.34	-490.65	-56.56
40	-4.41	-3.75	-7.04	-6.76	-395.15	-52.63	-535.09	-56.25
41	-5.12	-3.4	-9.53	-6.29	-428.46	-52.17	-537.81	-54.97
42	-5.41	-3.14	-11.21	-5.81	-526.74	-51.97	-460.73	-50.83
43	-3.63	-2.86	-5.4	-5.32	-534.24	-49.76	-314.71	-44.8
44	-2.34	-2.46	0.87	-4.79	-447.94	-45.34	-84.01	-37.21
45	-0.77	-2.04	6.28	-4.24	-263.28	-39.08	224.44	-28.45
46	1.88	-1.6	10.95	-3.71	27.76	-31.12	574.29	-19.21
47	5.29	-1.18	14.8	-3.24	404.74	-21.8	885.93	-10.72
48	9.37	-0.82	17.59	-2.86	796.92	-12.42	1079.86	-4.81
49	12.52	-0.57	18.99	-2.62	1099.94	-5.19	1076.64	-3.26
50	13.54	-0.48	19.26	-2.54	1213.03	-2.36	876.45	-6.6
51	12.27	-0.58	18.33	-2.63	1101.48	-5.08	547.09	-13.63
52	9.05	-0.84	16.47	-2.89	800.08	-12.21	177.83	-22.02
53	5.07	-1.21	13.65	-3.27	411.99	-21.39	-140.9	-29.8
54	1.32	-1.62	9.59	-3.75	38.93	-30.71	-360.92	-36.12
55	-1.08	-2.06	5.06	-4.28	-256.94	-38.81	-474.12	-40.59
56	-2.6	-2.48	0.01	-4.82	-444.68	-45.08	-467.21	-42.95
57	-3.81	-2.87	-5.47	-5.35	-532.37	-49.53	-347.76	-43.34
58	-5.24	-3.14	-10.27	-5.83	-529.49	-51.91	-242.87	-43.28
59	-4.7	-3.4	-7.8	-6.31	-436.05	-52.2	-234.55	-43.92
60	-3.64	-3.75	-4.79	-6.79	-400.69	-52.58	-299.79	-44.78
61	-3.76	-4.12	-2.71	-7.21	-443.31	-53.4	-375.85	-44.93
62	0.3	-4.46	7.67	-7.56	-436.19	-52.8	-380.88	-43.8
63	6.05	-4.77	21.37	-7.74	-351.19	-49.98	-299.73	-41.09
64	12.12	-5	32.22	-7.69	-248.04	-44.41	-204.44	-36.3
65	18.04	-5.07	34.9	-7.27	-152.13	-37.37	-120.12	-30.39
66	0	-5	0	-6.63	0	-30.29	0	-24.47

Table 3.12: FE results of chamber group 2 due to live load with one week modulus

Beam section no.	Dead load with one week creep modulus (DL3)			Live load at crown with one week creep modulus (LL3)			Live load at shoulder with one week creep modulus (LL4)		
	Vertical displ.	Bending moment	Thrust force	Vertical displ.	Bending moment	Thrust force	Vertical displ.	Bending moment	Thrust force
	mm	N-mm/mm	N/mm	mm	N-mm/mm	N/mm	mm	N-mm/mm	N/mm
34	-1.239	0	-6.53	-5.653	0	-30.07	-5.861	0	-34.61
35	-1.376	33.84	-7.18	-6.135	-146.03	-37.12	-6.478	-156.24	-42.09
36	-1.520	30.37	-7.6	-6.693	-238.68	-44.12	-7.145	-258.97	-49.24
37	-1.658	18.76	-7.67	-7.270	-339.07	-49.66	-7.873	-352.3	-54.2
38	-1.788	4.73	-7.51	-7.880	-421.64	-52.53	-8.616	-443.83	-56.45
39	-1.913	-5.33	-7.18	-8.536	-434.42	-53.34	-9.436	-490.65	-56.56
40	-2.032	-7.04	-6.76	-9.272	-395.15	-52.63	-10.354	-535.09	-56.25
41	-2.149	-9.53	-6.29	-10.117	-428.46	-52.17	-11.444	-537.81	-54.97
42	-2.265	-11.21	-5.81	-11.112	-526.74	-51.97	-12.696	-460.73	-50.83
43	-2.385	-5.4	-5.32	-12.335	-534.24	-49.76	-14.085	-314.71	-44.8
44	-2.504	0.87	-4.79	-13.784	-447.94	-45.34	-15.558	-84.01	-37.21
45	-2.622	6.28	-4.24	-15.450	-263.28	-39.08	-17.016	224.44	-28.45
46	-2.733	10.95	-3.71	-17.272	27.76	-31.12	-18.299	574.29	-19.21
47	-2.832	14.8	-3.24	-19.104	404.74	-21.8	-19.206	885.93	-10.72
48	-2.913	17.59	-2.86	-20.712	796.92	-12.42	-19.556	1079.86	-4.81
49	-2.966	18.99	-2.62	-21.823	1099.94	-5.19	-19.248	1076.64	-3.26
50	-2.987	19.26	-2.54	-22.217	1213.03	-2.36	-18.322	876.45	-6.6
51	-2.972	18.33	-2.63	-21.814	1101.48	-5.08	-16.933	547.09	-13.63
52	-2.924	16.47	-2.89	-20.694	800.08	-12.21	-15.296	177.83	-22.02
53	-2.852	13.65	-3.27	-19.075	411.99	-21.39	-13.630	-140.9	-29.8
54	-2.762	9.59	-3.75	-17.229	38.93	-30.71	-12.100	-360.92	-36.12
55	-2.663	5.06	-4.28	-15.390	-256.94	-38.81	-10.789	-474.12	-40.59
56	-2.559	0.01	-4.82	-13.708	-444.68	-45.08	-9.709	-467.21	-42.95
57	-2.452	-5.47	-5.35	-12.244	-532.37	-49.53	-8.803	-347.76	-43.34
58	-2.345	-10.27	-5.83	-11.009	-529.49	-51.91	-8.023	-242.87	-43.28
59	-2.240	-7.8	-6.31	-10.003	-436.05	-52.2	-7.336	-234.55	-43.92
60	-2.131	-4.79	-6.79	-9.146	-400.69	-52.58	-6.715	-299.79	-44.78
61	-2.017	-2.71	-7.21	-8.394	-443.31	-53.4	-6.158	-375.85	-44.93
62	-1.894	7.67	-7.56	-7.717	-436.19	-52.8	-5.661	-380.88	-43.8
63	-1.760	21.37	-7.74	-7.104	-351.19	-49.98	-5.206	-299.73	-41.09
64	-1.615	32.22	-7.69	-6.508	-248.04	-44.41	-4.780	-204.44	-36.3
65	-1.462	34.9	-7.27	-5.931	-152.13	-37.37	-4.366	-120.12	-30.39
66	-1.314	0	-6.63	-5.422	0	-30.29	-3.998	0	-24.47

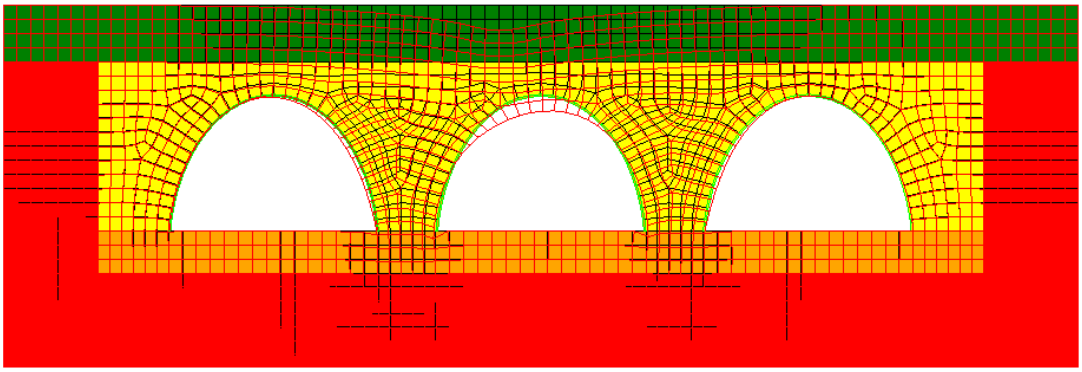

Figure 3.10: Deflection shape of the model under wheel load at shoulder of the middle arch

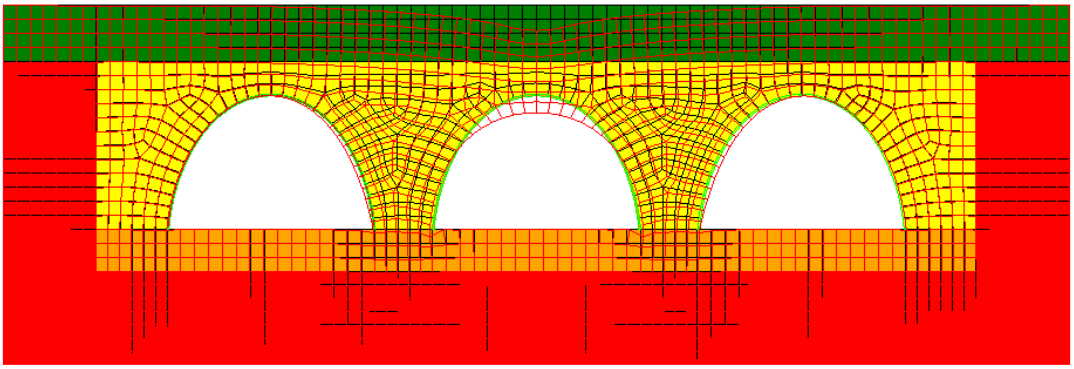

Figure 3.11: Deflection shape of the model under wheel load at the crown of the middle arch

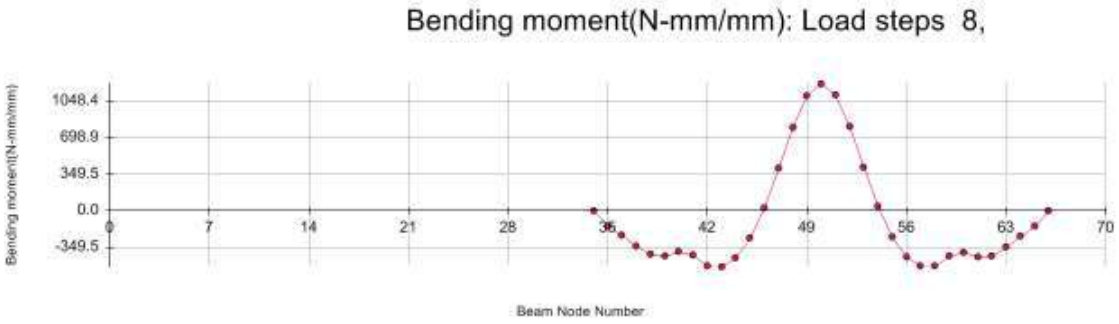

Figure 3.12: Bending moment diagram, analysis case LL1

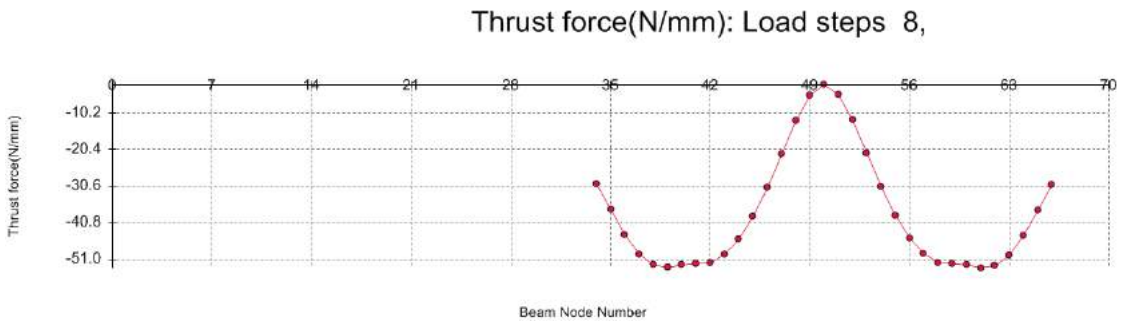

Figure 3.13: Thrust force diagram, analysis case LL1

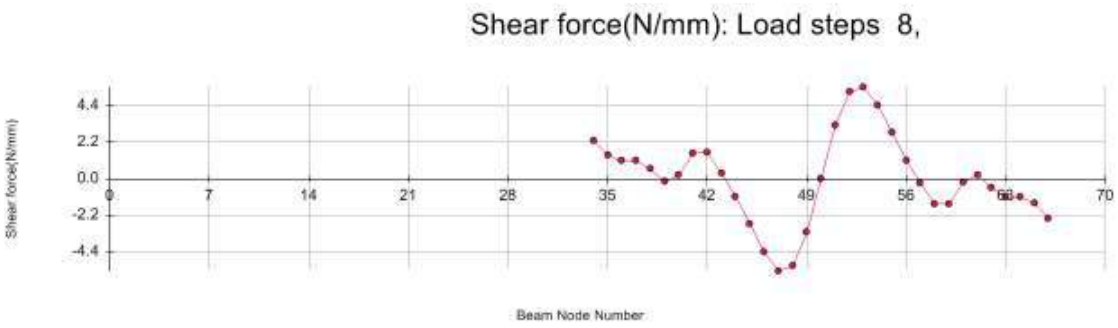

Figure 3.14: Shear force diagram, analysis case LL1

3.3 Post-processing

Structural adequacies were calculated in all beam cross-sections for all loading cases. The controlling beam sections were found according to the procedure outlined in the following sections. The procedure is presented here only for the controlling beam sections with the controlling load cases.

3.3.1 Short-term vehicle loading

Deflection

From Table 3.10 the maximum unfactored deflection due to long-term dead load is Δ_y = 3.491 mm, the chamber rise is 712 mm, thus Δ_y/D = 3.491/712 = 0.5%. This requirement is satisfied.

From Table 3.10 the maximum unfactored deflection due to live load is 20.365 – 2.110 = 18.255 mm. Allowable deflection of 2.5% of the rise is 17.80 mm. The requirement on deflection is slightly exceeded with an adequacy of 17.80/18.255 = 0.98.

Compression strength capacity (local buckling)

Compression strength is satisfied if the following equations are met (F 2787-09, Clause 8.3):

$$\frac{\varepsilon_{cy}}{\varepsilon_{Tf}} \geq 1, \text{ and } \frac{1.5\varepsilon_{cy}}{\varepsilon_{Mf}} \geq 1$$

where ε_{cy} is chamber thermoplastic compression yield strain; ε_{Tf} and ε_{Mf} are total factored compression strain due to thrust and due to combined thrust and bending, respectively.

Calculations of structural adequacy for local buckling due to axial thrust only and due to combined axial thrust and bending moment conditions are performed on all chamber sections to determine which sections are critical. The most critical chamber sections are the sections that have minimum adequacy.

Table 3.13 to Table 3.16 below present the results for the most critical chamber sections for the load case of short-term wheel load positioned over the crown (first case) and over the shoulder (second case).

Local buckling due to axial thrust only with short-term modulus

For axial thrust only, the critical sections are at beam section 40 (see Figure 3.9) due to short-term wheel loads at the crown and shoulder. Table 3.13 shows the finite element results extracted from Table 3.11. The factored hoop compression strain due to axial thrust is calculated as shown in

Table 3.14. Using the total factored hoop compression strain ε_c, the slenderness and effective width factors due to axial thrust only are calculated and tabulated in Table 3.15. The structural adequacies due to axial thrust only are calculated as shown in Table 3.16.

Table 3.13: Thrust forces at critical chamber sections, cover depth 460 mm

Location of wheel load	Crown	Shoulder	Formula
Beam section number	40	40	
Dead load with long-term creep modulus (N/mm)	3.750	3.750	$T_{DL.long}$
Dead load with short-term creep modulus (N/mm)	6.760	6.760	$T_{DL.short}$
Live load + dead load with short-term creep modulus (N/mm)	52.630	56.250	$T_{(DL+LL).short}$

Table 3.14: Average compressive strain in element due to axial thrust only, cover depth 460 mm

Location of wheel load	Crown	Shoulder	Formula
Beam section number	40	40	
Factored axial thrust due to LL with short-term creep modulus (N/mm)	82.566	89.082	$T_{short}= \gamma_{LL}(T_{(DL+LL).short}-T_{DL.short})$
Factored hoop compression strain due to LL with short-term modulus (mm/mm)	1.028E-02	1.109E-02	$\varepsilon_{c.short} = T_{short} / (E_{short}A_I)$
Factored axial thrust due to DL with long-term creep modulus (N/mm)	5.625	5.625	$T_{long}= \gamma_{DL}(T_{DL.long})$
Factored hoop compression strain due to DL with long-term modulus (mm/mm)	3.761E-06	3.761E-06	$\varepsilon_{c.long} = T_{long} / (E_{long}A_I)$
Total factored hoop compression strain (mm/mm)	1.028E-02	1.109E-02	$\varepsilon_c = \varepsilon_{c.short} + \varepsilon_{c.long}$

Table 3.15: Slenderness factor λ, effective width factor ρ, and effective area A_{eff} due to axial thrust only

Wheel load at crown	λ	ρ	A_{eff}
Element 1 (Figure 3.2)	0.963	0.801	
Element 2	0.649	1	7.505
Element 3	0.446	1	
Wheel load at shoulder	λ	ρ	A_{eff}
Element 1	1.000	0.780	
Element 2	0.674	1.000	7.446
Element 3	0.464	1	

The following formulae are used for slenderness factor λ, effective width factor ρ, and effective area A_{eff}:

$$\lambda_i = \left(\frac{w_i}{t_i}\right)\sqrt{\frac{\varepsilon_i}{k_i}} > 0.673 \qquad \rho_i = \frac{1-\frac{0.22}{\lambda_i}}{\lambda_i} \le 1 \qquad A_{eff} = (A_g - \sum n_i(1-\rho_i)w_i t_i) / period$$

in which w_i, t_i, k_i, and n_i are effective width, thickness, plate buckling edge support coefficient and number of elements per period, respectively, of the elements in the profile cross-section.

Table 3.16: Structural adequacy due to axial thrust only

Location of wheel load	Crown	Shoulder	Formula
Beam section number	40	40	
Hoop compression strain due to LL with short-term modulus (mm/mm)	1.100E-02	1.197E-02	$\varepsilon_{short} = T_{short} / (E_{short}A_{eff})$
Hoop compression strain due to DL with long-term modulus (mm/mm)	4.026E-03	4.058E-03	$\varepsilon_{long} = T_{long} / (E_{long}A_{eff})$
Total hoop compression strain (mm/mm)	1.503E-02	1.602E-02	$\varepsilon_{Tf} = \varepsilon_{short} + \varepsilon_{long}$
Specified limiting compression strain ε_{cy} (mm/mm)	3.300E-02	3.300E-02	*
Adequacy due to thrust only	**2.20**	**2.06**	$\varepsilon_{cy} / \varepsilon_{Tf}$

Note: * Provided by Cubic Solutions and is consistent with the examples provided in the ASTM F2787-09.

Local buckling due to combined thrust and bending with short-term modulus

Following a similar procedure to the thrust-only case, the minimum structural adequacies due to combined thrust and bending moment are found to occur in beam section number 40.

Table 3.17 shows the finite element results extracted from Table 3.11 for the controlling beam sections. The factored axial thrust and bending moments, and thrust strain at these sections are calculated in Table 3.18. The factored compression strains due to bending and combined thrust and bending at the valley and crest are calculated as shown in Table 3.18. Table 3.19 summarises the factored compression strain due to combined thrust and bending at valley and crest. Using the total factored compression strains $\varepsilon_{c,\,valley}$ and $\varepsilon_{c,\,crest}$, the slenderness and effective width factors are recalculated and tabulated in Table 3.20 and Table 3.22, respectively. The structural adequacies due to combined axial thrust and bending moment are calculated as shown in Table 3.21 and Table 3.23, respectively for valley and crest.

Table 3.17: Finite element results due to combined axial thrust and bending

Location of wheel load	Crown	Shoulder	Formula
Beam section number	40	40	
Dead load with long-term creep modulus	DL2	DL2	
Axial thrust	3.750	3.750	$T_{DL.long}$
Bending moment	4.410	4.410	$M_{DL.long}$
Dead load with short-term creep modulus	DL1	DL1	
Axial thrust	6.760	6.760	$T_{DL.short}$
Bending moment	7.040	7.040	$M_{DL.short}$
Live load + Dead load with short-term creep modulus (N/mm)	LL1	LL2	
Axial thrust	52.630	56.250	$T_{(DL+LL).short}$
Bending moment	395.150	535.090	$M_{(DL+LL).short}$

Table 3.18: Average compressive strain in element due to combined axial thrust and bending

Location of wheel load	Crown	Shoulder	Formula
Beam section number	40	40	
Short-term load component only			
Factored axial thrust due to LL with short-term creep modulus (N/mm)	82.566	89.082	$T_{short} = \gamma_{LL}(T_{(DL+LL).short} - T_{DL.short})$
Factored bending moment due to LL with short-term	698.598	950.490	$M_{short} = \gamma_{LL}(M_{(DL+LL).short} - M_{DL.short})$

creep modulus (N-mm/mm)			
Factored hoop compression strain due to LL with short-term modulus (mm/mm)	1.028E-02	1.109E-02	$\varepsilon_{c.short} = T_{short} / (E_{short}A_l)$
Long-term load component only			
Factored axial thrust due to DL with long-term creep modulus (N/mm)	5.625	5.625	$T_{long} = \gamma_{DL}(T_{DL.long})$
Factored bending moment due to DL with long-term creep modulus (N-mm/mm)	6.615	6.615	$M_{long} = \gamma_{DL}(M_{DL.long})$
Factored hoop compression strain due to DL with long-term modulus (mm/mm)	3.761E-03	3.761E-03	$\varepsilon_{c.long} = T_{long} / (E_{long}A_l)$
Total factored hoop compression strain (mm/mm)	1.404E-02	1.485E-02	$\varepsilon_c = \varepsilon_{c.short} + \varepsilon_{c.long}$

Table 3.19: Factored compression strain due to combined thrust and bending at valley and crest

Location of wheel load	Crown	Shoulder	Formula
Beam section number	40	40	
Strain at valley outer fiber due to short-term loading	4.209E-03	5.727E-03	$\varepsilon_{valley.short} = M_{short}\, y_v / (E_{short}I_l)$
Strain at crest outer fiber due to short-term loading	5.882E-03	8.003E-03	$\varepsilon_{crest.short} = M_{short}\, y_c / (E_{short}I_l)$
Strain at valley outer fiber due to long-term loading	2.141E-04	2.141E-04	$\varepsilon_{valley.long} = M_{long}\, y_v / (E_{long}I_l)$
Strain at crest outer fiber due to long-term loading	1.701E-07	1.701E-07	$\varepsilon_{crest.long} = M_{long}\, y_c / (E_{long}I_l)$
Strain due to bending at valley	4.423E-03	5.941E-03	$\varepsilon_{valley} = \varepsilon_{valey.long} + \varepsilon_{valley.short}$
Strain due to bending at crest	5.882E-03	8.003E-03	$\varepsilon_{crest} = \varepsilon_{crest.long} + \varepsilon_{crest.short}$
Total factored compression strain at valley	1.846E-02	2.079E-02	$\varepsilon_{c.valley} = \varepsilon_c + \varepsilon_{valley}$
Total factored compression strain at crest	1.992E-02	2.286E-02	$\varepsilon_{c.crest} = \varepsilon_c + \varepsilon_{crest}$

Table 3.20: Slenderness factor λ, effective width factor ρ, and effective area A_{eff} calculated at valley

Wheel load at crown	λ	ρ	$A_{eff.TM}$
Element 1 (Figure 3.2)	1.290	0.643	
Element 2	0.870	0.859	6.579
Element 3	0.598	1	
Wheel load at shoulder	λ	ρ	$A_{eff.TM}$
Element 1	1.369	0.613	
Element 2	0.923	0.825	6.379
Element 3	0.635	1	

Table 3.21: Calculation of structural adequacies due to combined axial thrust and bending at valley

Location of wheel load	Crown	Shoulder	Formula
Beam section number	40	40	
Hoop compression strain due to LL with short-term modulus (mm/mm)	1.255E-02	1.295E-02	$\varepsilon_{short} = T_{short} / (E_{short}A_{eff.TM})$
Hoop compression strain due to DL with long-term modulus (mm/mm)	4.593E-03	4.737E-03	$\varepsilon_{long} = T_{long} / (E_{long}A_{eff.TM})$
Total hoop compression strain (mm/mm)	1.715E-02	1.768E-02	$\varepsilon_{Mf} = \varepsilon_{short} + \varepsilon_{long}$
Specified limiting compression strain εcy (mm/mm)	3.300E-02	3.300E-02	
Adequacy due to combined axial thrust and bending at valley	**2.89**	**2.80**	$1.5\varepsilon_{cy} / \varepsilon_{Mf}$

Table 3.22: Slenderness factor λ, effective width factor ρ, and effective area A_{eff} calculated at crest

Wheel load at crown	λ	ρ	$A_{eff.TM}$
Element 1 (Figure 3.2)	1.340	0.624	
Element 2	0.903	0.83737309	6.451
Element 3	0.621	1	
Wheel load at shoulder	λ	ρ	$A_{eff.TM}$
Element 1	1.436	0.590	
Element 2	0.968	0.79851436	6.221
Element 3	0.666	1	

Table 3.23: Calculation of structural adequacies due to combined axial thrust and bending at crest

Location of wheel load	**Crown**	**Shoulder**	**Formula**
Beam section number	40	40	
Hoop compression strain due to LL with short-term modulus (mm/mm)	1.280E-02	1.327E-02	$\varepsilon_{short} = T_{short} / (E_{short}A_{eff.TM})$
Hoop compression strain due to DL with long-term modulus (mm/mm)	4.684E-03	4.857E-03	$\varepsilon_{long} = T_{long} / (E_{long}A_{eff.TM})$
Total hoop compression strain (mm/mm)	1.749E-02	1.813E-02	$\varepsilon_{Mf} = \varepsilon_{short} + \varepsilon_{long}$
Specified limiting compression strain εcy (mm/mm)	3.300E-02	3.300E-02	*
Adequacy due to combined axial thrust and bending at crest	**2.83**	**2.73**	$1.5\varepsilon_{cy} / \varepsilon_{Mf}$

Note: * Provided by Cubic Solutions and is consistent with the examples provided in the ASTM F2787-09.

Global buckling capacity

According to ASTM F2787-09, at any given wall cross-section, the critical buckling thrust T_{CR}, shall be greater than the maximum factored thrust due to dead and live loads T, i.e. $T_{CR}/T \geq 1$. These values are calculated by the following formulae:

$$T_{CR} = \frac{1.2C_n(E_L I)^{0.33}(\phi_s M_s k_v)^{0.67} R_h}{FS} \qquad k_v = \frac{(1+\nu)(1-2\nu)}{1-\nu} \qquad R_h = \frac{11.4}{11+D/h}$$

$T = \gamma_{DL}T_{DL} + \gamma_{LL}T_{LL}$, in which

$T_{DL} = T_{DL\_long}$ and $T_{LL} = T_{(DL+LL).short} - T_{DL.short}$

Details of the parameters used in the above formulae are shown in Table 3.24.

Table 3.24: Parameters for global buckling calculation

Name	**Description**	**Value**
FS	Design factor, =2.5	2.5
C_n	Scalar calibration factor to account for nonlinear effects, = 0.55	0.55
ϕ_s	Strength reduction factor for soil, =0.9	0.9
k_v	Coefficient, k_v = 0.74 for the soil poisson's ratio of 0.3	0.74
Ms	Constrained soil modulus (MPa), assumed Sn-90, stress level 0.21 ksf	8.946
E_L	50 yr creep modulus (Mpa)	186
I	Moment of inertia of the chamber wall cross-section (mm^4/mm)	4837.73
D	Nominal span of chamber (mm)	1295

h	Height of soil cover over the chamber (mm)	460
R_h	Chamber geometry parameter	0.825

From the above equations, due to wheel load at the crown, the critical buckling thrust T_{CR} (N/mm) is 391.89 and the maximum factored thrust due to dead loads with long-term modulus and live loads with short-term modulus T (N/mm) is 88.191 at beam section 40. Thus the global buckling adequacy is 4.44.

Similar calculations were performed for the case of wheel load at the shoulder gave a global buckling adequacy of 4.14.

It can be derived from the above results that, except for the deflection, it is critical when live load is at the shoulder (quarter of the chamber span). This observation is always true for subsequent analysis cases in this report.

3.3.2 One week parking vehicle

No dynamic load allowance is added to live load in this case as it can be assumed that the vehicle is parked for one week.

A similar procedure was used to evaluate the chamber's capacity in terms of deflection, local buckling and global buckling. Results are presented below.

Deflection

The maximum unfactored deflection due to live load is 22.217 – 2.987 = 19.230 mm. Allowable deflection of 2.5% of the rise is 17.80 mm. The requirement on deflection is exceeded with an adequacy of 17.80/19.23 = 0.93.

Local buckling due to axial thrust only

Table 3.25: Thrust forces at critical chamber sections, 460 mm cover depth

Location of wheel load	Crown	Shoulder	Formula
Beam section number	40	40	
Dead load with long-term creep modulus (N/mm.)	3.750	3.750	$T_{DL.long}$
Dead load with 1 week creep modulus (N/mm.)	4.720	4.720	$T_{DL.short}$
Live load + dead load with 1 week creep modulus (N/mm.)	31.790	35.400	$T_{(DL+LL).short}$

Table 3.26: Average compressive strain in element due to axial thrust only

Location of wheel load	Crown	Shoulder	Formula
Beam section number	40	40	
Factored axial thrust due to LL with 1 week creep modulus (N/mm)	48.726	55.224	$T_{short}= \gamma_{LL}(T_{(DL+LL).short}-T_{DL.short})$
Factored hoop compression strain due to LL with 1 week modulus (mm/mm)	1.955E-02	2.215E-02	$\varepsilon_{c.short} = T_{short} / (E_{short}A_l)$
Factored axial thrust due to DL with long-term creep modulus (N/mm)	5.625	5.625	$T_{long}= \gamma_{DL}(T_{DL.long})$
Factored hoop compression strain due to DL with long-term modulus (mm/mm)	3.761E-06	3.761E-06	$\varepsilon_{c.long} = T_{long} / (E_{long}A_l)$
Total factored hoop compression strain (mm/mm)	1.955E-02	2.216E-02	$\varepsilon_c = \varepsilon_{c.short} + \varepsilon_{c.long}$

Table 3.27: Slenderness factor λ, effective width factor ρ, and effective area A_{eff} due to axial thrust only

Wheel load at crown	λ	ρ	A_{eff}
Element 1 (Figure 3.2)	1.328	0.628	
Element 2	0.895	0.843	6.482
Element 3	0.616	1	
Wheel load at shoulder	λ	ρ	A_{eff}
Element 1	1.414	0.597	
Element 2	0.953	0.807	6.273
Element 3	0.655	1	

Table 3.28: Structural adequacy due to axial thrust only

Location of wheel load	**Crown**	**Shoulder**	**Formula**
Beam section number	40	40	
Hoop compression strain due to LL with 1 week modulus (mm/mm)	2.423E-02	2.838E-02	$\varepsilon_{short} = T_{short} / (E_{short}A_{eff})$
Hoop compression strain due to DL with long-term modulus (mm/mm)	4.661E-03	4.817E-03	$\varepsilon_{long} = T_{long} / (E_{long}A_{eff})$
Total hoop compression strain (mm/mm)	2.889E-02	3.319E-02	$\varepsilon_{Tf} = \varepsilon_{short} + \varepsilon_{long}$
Specified limiting compression strain ε_{cy} (mm/mm)	3.300E-02	3.300E-02	*
Adequacy due to thrust only	**1.14**	**0.99**	$\varepsilon_{cy} / \varepsilon_{Tf}$

Note: * Provided by Cubic Solutions and is consistent with the examples provided in the ASTM F2787-09.

Local buckling due to combined thrust and bending

Table 3.29: Finite element results due to combined axial thrust and bending

Location of wheel load	**Crown**	**Shoulder**	**Formula**
Beam section number	40	40	
Dead load with long-term creep modulus	DL2	DL2	
Axial thrust	3.750	3.750	$T_{DL.long}$
Bending moment	4.410	4.410	$M_{DL.long}$
Dead load with 1 week creep modulus	DL1	DL1	
Axial thrust	4.720	4.720	$T_{DL.short}$
Bending moment	5.410	5.410	$M_{DL.short}$
Live load + dead load with 1 week creep modulus (N/mm)	LL1	LL2	
Axial thrust	31.790	35.400	$T_{(DL+LL).short}$
Bending moment	150.460	197.610	$M_{(DL+LL).short}$

Table 3.30: Average compressive strain in element due to combined axial thrust and bending

Location of wheel load	**Crown**	**Shoulder**	**Formula**
Beam section number	40	40	
Short-term load component only			
Factored axial thrust due to LL with 1 week creep modulus (N/mm)	48.726	55.224	$T_{short} = \gamma_{LL}(T_{(DL+LL).short} - T_{DL.short})$
Factored bending moment due to LL with 1 week creep modulus (N-mm/mm)	261.090	345.960	$M_{short} = \gamma_{LL}(M_{(DL+LL).short} - M_{DL.short})$

Factored hoop compression strain due to LL with 1 week modulus (mm/mm)	1.955E-02	2.215E-02	$\varepsilon_{c.short} = T_{short} / (E_{short}A_I)$
Long-term load component only			
Factored axial thrust due to DL with long-term creep modulus (N/mm)	5.625	5.625	$T_{long} = \gamma_{DL}(T_{DL.long})$
Factored bending moment due to DL with long-term creep modulus (N-mm/mm)	6.615	6.615	$M_{long} = \gamma_{DL}(M_{DL.long})$
Factored hoop compression strain due to DL with long-term modulus (mm/mm)	3.761E-03	3.761E-03	$\varepsilon_{c.long} = T_{long} / (E_{long}A_I)$
Total factored hoop compression strain (mm/mm)	2.331E-02	2.592E-02	$\varepsilon_c = \varepsilon_{c.short} + \varepsilon_{c.long}$

Table 3.31: Factored compression strain due to combined thrust and bending at valley and crest

Location of wheel load	Crown	Shoulder	Formula
Beam section number	40	40	
Strain at valley outer fiber due to 1 week loading	5.069E-03	6.717E-03	$\varepsilon_{valley.short} = M_{short}\, y_v / (E_{short}I_I)$
Strain at crest outer fiber due to 1 week loading	7.084E-03	9.386E-03	$\varepsilon_{crest.short} = M_{short}\, y_c / (E_{short}I_I)$
Strain at valley outer fiber due to long-term loading	2.141E-04	2.141E-04	$\varepsilon_{valley.long} = M_{long}\, y_v / (E_{long}I_I)$
Strain at crest outer fiber due to long-term loading	1.701E-07	1.701E-07	$\varepsilon_{crest.long} = M_{long}\, y_c / (E_{long}I_I)$
Strain due to bending at valley	5.283E-03	6.931E-03	$\varepsilon_{valley} = \varepsilon_{valey.long} + \varepsilon_{valley.short}$
Strain due to bending at crest	7.084E-03	9.386E-03	$\varepsilon_{crest} = \varepsilon_{crest.long} + \varepsilon_{crest.short}$
Total factored compression strain at valley	2.859E-02	3.285E-02	$\varepsilon_{c.valley} = \varepsilon_c + \varepsilon_{valley}$
Total factored compression strain at crest	3.039E-02	3.530E-02	$\varepsilon_{c.crest} = \varepsilon_c + \varepsilon_{crest}$

Table 3.32: Slenderness factor λ, effective width factor ρ, and effective area A_{eff} calculated at valley

Wheel load at crown	λ	ρ	$A_{eff.TM}$
Element 1 (Figure 3.2)	1.606	0.537	
Element 2	1.082	0.736	5.793
Element 3	0.744	0.946	
Wheel load at shoulder	λ	ρ	$A_{eff.TM}$
Element 1	1.721	0.507	
Element 2	1.160	0.699	5.529
Element 3	0.798	0.908	

Table 3.33: Calculation of structural adequacies due to combined axial thrust and bending at valley

Location of wheel load	Crown	Shoulder	Formula
Beam section number	40	40	
Hoop compression strain due to LL with 1 week modulus (mm/mm)	2.711E-02	2.840E-02	$\varepsilon_{short} = T_{short} / (E_{short}A_{eff.TM})$
Hoop compression strain due to DL with long-term modulus (mm/mm)	5.216E-03	5.465E-03	$\varepsilon_{long} = T_{long} / (E_{long}A_{eff.TM})$
Total hoop compression strain (mm/mm)	3.233E-02	3.387E-02	$\varepsilon_{Mf} = \varepsilon_{short} + \varepsilon_{long}$
Specified limiting compression strain εcy (mm/mm)	3.300E-02	3.300E-02	*
Adequacy due to combined axial thrust and bending at valley	**1.53**	**1.46**	$1.5\varepsilon_{cy} / \varepsilon_{Mf}$

Note: * Provided by Cubic Solutions and is consistent with the examples provided in the ASTM F2787-09.

Table 3.34: Slenderness factor λ, effective width factor ρ, and effective area A_{eff} calculated at crest

Wheel load at crown	λ	ρ	$A_{eff.TM}$
Element 1 (Figure 3.2)	1.656	0.524	
Element 2	1.116	0.720	5.676
Element 3	0.768	0.929	
Wheel load at shoulder	λ	ρ	$A_{eff.TM}$
Element 1	1.784	0.491	
Element 2	1.203	0.679	5.394
Element 3	0.827	0.887	

Table 3.35: Calculation of structural adequacies due to combined axial thrust and bending at crest

Location of wheel load	**Crown**	**Shoulder**	**Formula**
Beam section number	40	40	
Hoop compression strain due to LL with 1 week modulus (mm/mm)	2.767E-02	2.911E-02	$\varepsilon_{short} = T_{short} / (E_{short}A_{eff.TM})$
Hoop compression strain due to DL with long-term modulus (mm/mm)	5.324E-03	5.602E-03	$\varepsilon_{long} = T_{long} / (E_{long}A_{eff.TM})$
Total hoop compression strain (mm/mm)	3.299E-02	3.472E-02	$\varepsilon_{Mf} = \varepsilon_{short} + \varepsilon_{long}$
Specified limiting compression strain εcy (mm/mm)	3.300E-02	3.300E-02	*
Adequacy due to combined axial thrust and bending at crest	**1.50**	**1.43**	$1.5\varepsilon_{cy} / \varepsilon_{Mf}$

Note: * Provided by Cubic Solutions and is consistent with the examples provided in the ASTM F2787-09.

Global buckling capacity

Using similar formulae and parameters as in Section 3.3.1 for calculation of global buckling capacity, the global buckling adequacy is 7.21 for the case of wheel load placed at the crown and 6.44 for the case of wheel load placed at the shoulder.

Summary of structural adequacies

Table 3.36: Summary of structural adequacies, 460 mm cover depth

Load combination	**Short term creep modulus**		**One week creep modulus**	
	Live load at crown	Live load at shoulder	Live load at crown	Live load at shoulder
Deflection due to live load	0.98	1.05	0.93	1.07
Axial thrust only	2.20	2.06	1.14	0.99
Combined axial thrust and bending moment	2.83	2.73	1.50	1.43
Global buckling	4.44	4.14	7.21	6.44

From Table 3.36, it can be noted that the controlling structural adequacy is 0.93 for the case of short-term deflection. The safety margins of other quantities are small. Thus, it is recommended that the cover depth above the chamber be increased to 600 mm to account for rutting due to vehicle impacts.

3.4 Calculation of Bearing Pressure

The bearing of the chamber foot on the foundation and of the foundation on the subgrade, due to live load and soil weight is calculated in this section. Consider a chamber with cover height between 600 mm and 3600 mm. The minimum foundation thickness of 230 mm (9 in.) is investigated. The soil density is assumed to be 1900 kg/m^3.

Contribution of live load to the bearing at the foundation is highest when the axle is centered between two adjacent chambers as in Figure 3.14. The wheel load is distributed through fill in accordance with the AS 5100 specification. In the calculation, the live load is distributed out-of-plane and checked for interaction between the two wheels of the axle. If the effective load width after live load distribution exceeds the crown-to-crown spacing, the fraction of wheel load that is transferred through the soil between two chambers is calculated by multiplying the effective pressure at the crown level with the crown-to-crown spacing. This represents the distribution of some of the live load away from the soil between two chambers.

Live load is distributed to the chamber crown level for calculating the bearing on the foundation below the chamber foot. For the live load contribution to the subgrade, further distribution through the chamber and foundation thickness is calculated. Dynamic load allowance is included.

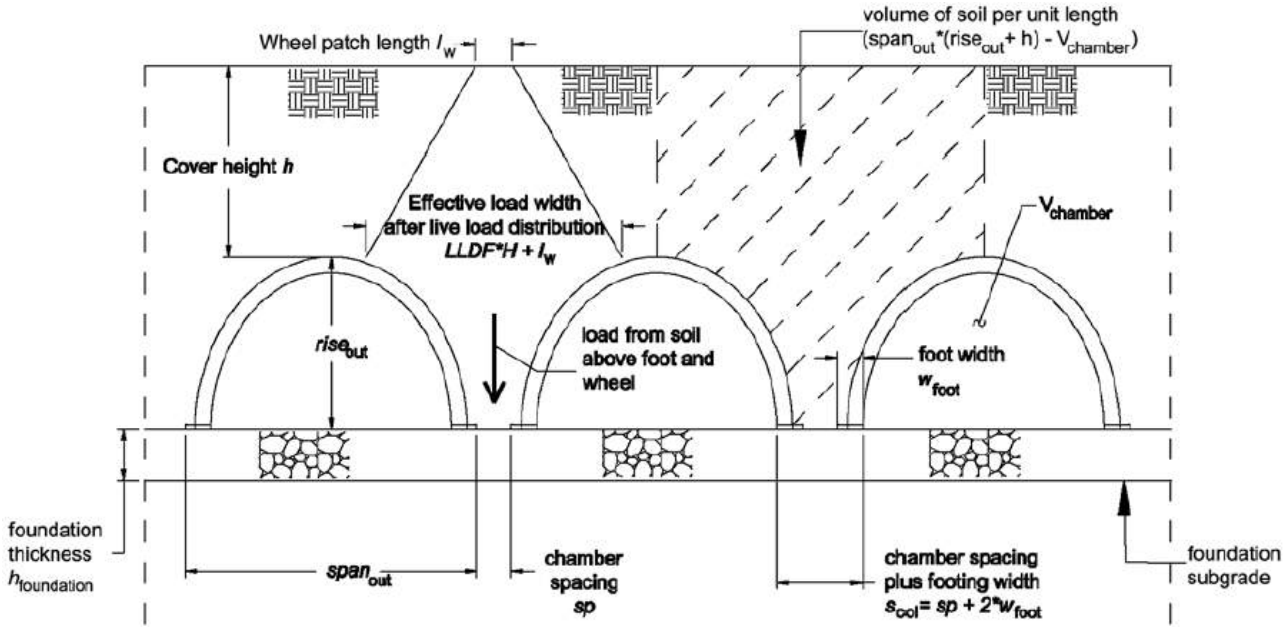

Figure 3.15: Schematic of bearing problem

Source: ASTM F2787-09.

Various cover heights in the range of 460 mm to 3600 mm are investigated. The following procedure shows the calculations for the case of 460 mm cover height.

Table 3.37 presents the parameters of chamber geometry for the foundation bearing calculation. Live load data for the W80 and A160 loads is presented in Table 3.38.

Table 3.37: Chamber geometry for foundation bearing calculation

Chamber geometry	Value	Unit	Denotation	Formula
Span (outside of foot-to outside of foot)	1295	mm	span_out	
Distance from outside of foot to centre of gravity of foot	115	mm	w_foot	
Adjacent chamber spacing	152	mm	sp	
Soil column width	267	mm	s_col	s_col = sp + 2 w_foot
Outside rise	762	mm	rise_out	
Crown-to-crown spacing	1448	mm	sp_crown	sp_crown=span_out + sp
Chamber storage volume per unit length	568,000	mm^3/mm	V_chamber	
Soil design unit weight	1900	kg/m^3	γ	
Foundation thickness	229	mm	h_found	
Cover height	460	mm	He	

Table 3.38: Live load parameters for foundation bearing calculation

Live load parameters	Value	Unit	Denotation
Axle load	160	kN	F_axle
Wheel contact length	250	mm	L_w
Wheel contact width	400	mm	W_w
Axial width (distance between tyres)	2000	mm	axle
Accompanying lane factor	1	--	mpf
Dynamic load allowance	0.4	--	IM
Impact factor	1.331	--	I_imp

The in-plane live load distribution is determined in such a way that if the effective load width after live load distribution exceeds the crown-to-crown spacing, the wheel live load should be recalculated using the crown-to-crown spacing. Results are presented in Table 3.39.

Table 3.39: In-plane live load distribution

Item	Value	Unit	Denotation	Formula
Axle load, including accompanying lane factor and dynamic load allowance	213.019	kN	F	F=mpf*F_axle*I_imp
Dead load on foundation	22.311	kN/m	DL	DL=γ(sp_crown (rise_out + h)) - V_chamber)
Wheel load equivalent distribution width at the chamber crown	658.640	mm	W_eff	W_eff=L_w + 100mm+1.2*(He-200mm)
Effective live load pressure at the chamber crown	161.711	kN/m	P_crown	P_crown = 0.5 F/W_eff
In-plane live load distribution through the 'soil column' between two adjacent chambers	106.509	kN	LL_in	LL_in = P_crown * W_eff if W_eff <=sp_crown, otherwise LL_in = P_crown * sp_crown

The out-of-plane live load distributions are shown in Table 3.40 for the foundation level and Table 3.41 for the subgrade level.

Table 3.40: Out-of-plane live load distribution on foundation

Item	Value	Unit	Denotation	Formula
Depth at which wheels on an axle interact	1450	mm	D_axle	D_axle = (axle - W_w+140)/1.2
Depth to foundation	1219	mm	D_found	D_found = He + rise_out
Depth to subgrade	1448	mm	D_subgrade	D_subgrade = D_found + h_found
Wheel load distribution length at foundation level (no overlap)	1723	mm	W_wheelF	W_wheelF = W_w + 100mm+1.2*(D_found-200mm)
Axle load distribution length at foundation level (overlap)	3723	mm	W_axleF	W_axleF = axle + W_w + 100mm+1.2*(D_found-200mm)
Wheel live load equivalent distribution (no overlap)	61.815	kN/m	LL_found_wheel	LL_found_wheel = LL_in.plane.scaled / W_wheelF
Axle live load equivalent distribution (overlap)	57.216	kN/m	LL_found_axle	LL_found_axle = 2*LL_in.plane.scaled / W_axleF
Determine controlling distribution (wheel load)	61.815	kN/m	LL_found	=LL_found_wheel if D_found < D_axle, otherwise, LL_found_axle

Table 3.41: Out-of-plane live load distribution on subgrade

Item	Value	Unit	Denotation	Formula
Wheel load distribution length at foundation level (no overlap)	1997.36	mm	W_wheelS	W_wheelS = W_w + 100mm+1.2*(D_subgrade-200mm)
Axle load distribution length at foundation level (overlap)	3997.36	mm	W_axleS	W_axleS = axle + W_w + 100mm+1.2*(D_subgrade-200mm)
Wheel live load equivalent distribution (no overlap)	53.325	kN/m	LL_sub_wheel	LL_sub_wheel = LL_in.plane.scaled / W_wheelS
Axle live load equivalent distribution (overlap)	53.290	kN/m	LL_sub_axle	=2*LL_in.plane.scaled / W_axleS
Determine controlling distribution (axle load)	53.290	kN/m	LL_subgrade	=LL_sub_wheel if D_found < D_axle, otherwise, LL_sub_axle

The above calculations are calculated for all cover heights from 460 mm (1.5 ft) to 3660 mm (12 ft). The total load distribution on foundation and on subgrade is summarised in Table 3.42.

Table 3.42: Total load distribution on foundation and on subgrade (unfactored)

Cover height	Dead load	On foundation		On subgrade	
		Live load	Total load	Live load	Total load
mm	kN/m	kN/m	kN/m	kN/m	kN/m
460	22.31	61.81	84.12	53.29	75.60
610	26.42	54.92	81.34	50.08	76.51
914	34.64	47.30	81.94	44.44	79.09
1219	42.87	41.99	84.86	39.65	82.51
1524	51.09	37.46	88.55	35.51	86.60

1829	59.31	33.54	92.85	31.91	91.23
2134	67.53	30.69	98.22	29.29	96.82
2438	75.76	28.85	104.61	27.61	103.36
2743	83.98	27.22	111.20	26.11	110.09
3048	92.20	25.76	117.96	24.77	116.97
3353	100.42	24.45	124.87	23.55	123.98
3660	108.65	23.27	131.92	22.45	131.10

The maximum values of total load distribution on foundation and on subgrade are used to evaluate the bearing capacity of the foundation and subgrade. Assuming that the ultimate bearing capacities of foundation stone and subgrade soil are 1341 kPa and 100 kPa, respectively, the safety factors are presented in Table 3.43 for the foundation and Table 3.44 for the subgrade, respectively.

Table 3.43: Evaluation of bearing on foundation below chamber foot

Item	Value	Unit	Denotation	Formula
Total load on foundation	131.92	kN/m	TotalLoad_found	TotalLoad_found = DL + LL_found
Assumed ultimate bearing capacity of foundation stone	1341	kPa	q_u.found	---
Pressure on foundation below chamber foot	493	kPa	P_f	P_f = TotalLoad_found / s_col
Factor of safety	2.72	---	FS_found	FS_found = q_u.found/P_f

Table 3.44: Evaluation of bearing on subgrade below the foundation

Item	Value	Unit	Denotation	Formula
Total load on subgrade	131.10	kN/m	TotalLoad_subgrade	TotalLoad_subgrade = DL + LL_subgrade
Assumed allowable bearing capacity of subgrade soil	100	kPa	q_u.subgrade	
Effective subgrade load width	542	mm	W_eff.subgrade	W_eff.subgrade = s_col + 1.2*h_found
Pressure on subgrade	246	kPa	p_subgrade	p_subgrade = TotalLoad_subgrade / W_eff.subgrade + γ * h_found

It should be noted that load will be distributed through the foundation layer on an angle of 30 degrees (1.2 h). The safety factor for the foundation is 2.72, which is less than the recommended value of 3.0. Further calculations show that the ultimate bearing capacity of the foundation should be 1.5 MPa to obtain a safety factor of 3.0.

At the minimum specified depth of the foundation layer according to the StormTech manual, the required allowable bearing capacity of subgrade soil needs to be 250 kPa. Further investigations showed that if the thickness of the foundation layer is 500 mm, the required allowable bearing capacity of subgrade soil needs to be 160 kPa.

4 SENSITIVITY ANALYSIS

4.1 Effect of Cover Depth

4.1.1 Minimum cover depth

As shown in Section 2, with a cover depth of 460 mm for the one week live load case, the chamber capacity against the short-term deflection and axial thrust was slightly exceeded.

Two models have been analysed in which the cover depth was increased to 610 mm and 760 mm, respectively. Table 4.1 shows the summary of structural adequacies for the cover depth of 610 mm, and Table 4.2 for the cover depth of 760 mm.

Table 4.1: Structural adequacies for 610 mm cover depth

Load combination	Short-term creep modulus		One week creep modulus	
	Live load at crown	Live load at shoulder	Live load at crown	Live load at shoulder
Deflection due to live load	1.50	1.55	1.31	1.45
Axial thrust only	2.70	2.50	1.45	1.34
Combined axial thrust and bending moment	3.53	3.42	1.88	1.83
Global buckling	6.63	6.02	9.43	8.88

Table 4.2: Structural adequacies for 760 mm cover depth

Load combination	Short-term creep modulus		One week creep modulus	
	Live load at crown	Live load at shoulder	Live load at crown	Live load at shoulder
Deflection due to live load	1.83	2.02	1.70	1.85
Axial thrust only	2.80	2.78	1.71	1.66
Combined axial thrust and bending moment	3.62	3.60	2.17	2.15
Global buckling	8.17	8.06	11.48	11.24

It can be concluded from Table 3.36, Table 4.1 and Table 4.2 that the structural adequacies of the chamber are improved when the cover depth is increased. The results are graphically presented in Figure 4.1, where the variation of adequacies due to global buckling vs. cover depth is omitted because of its high safety margins. It can be derived from this figure that the minimum cover depth, with which the chamber satisfies all structural requirements, is 470 mm.

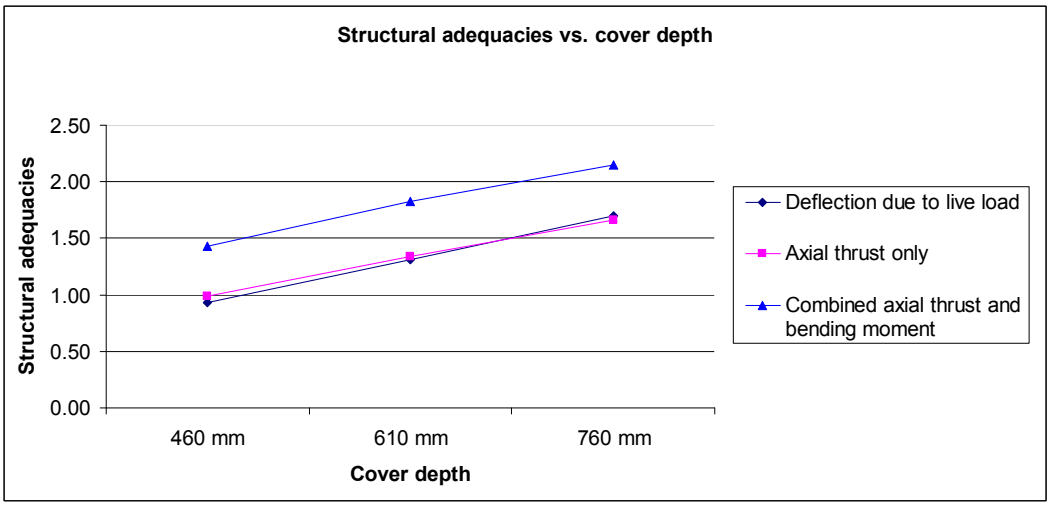

Figure 4.1: Structural adequacies vs. cover depth

4.1.2 Maximum cover depth

In order to determine the maximum allowable cover depth, a model with 3660 mm (12 ft) cover depth was analysed. It is noted that all soil layers above the cover depth of 460 mm are modelled using the SW90 soil type (Table 3.5).

Investigations show that the load effects of M1600 govern at the maximum depth. Dynamic load allowance is included for the short-term loading case. Thus M1600 load is used for this analysis. Similar to shallow cases, two live load locations are considered, including the middle axle at the crown and the middle axle at the shoulder as shown in Figure 4.2.

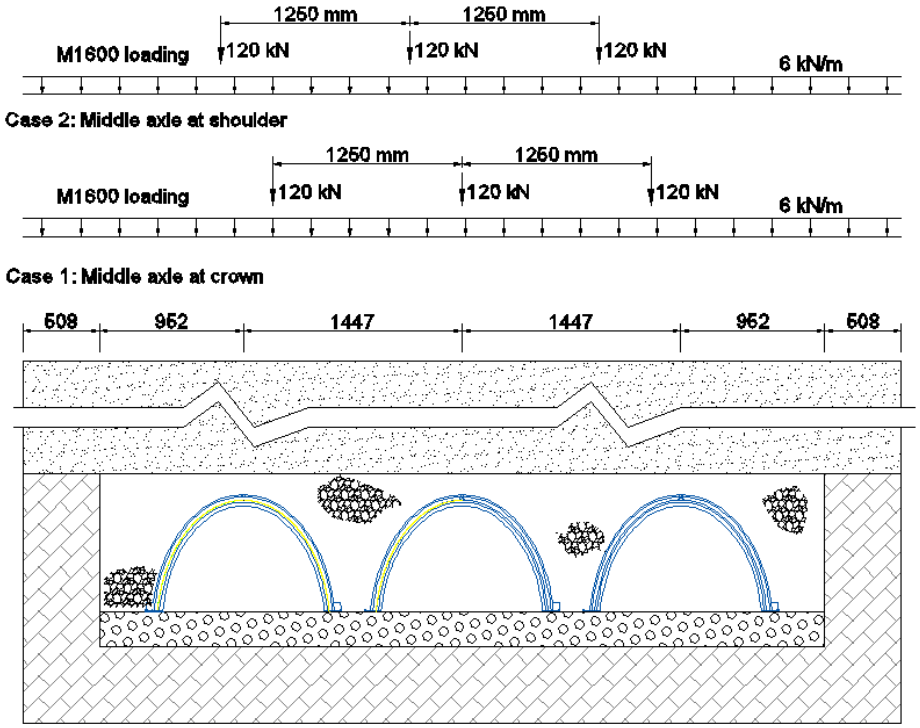

Figure 4.2: M1600 load cases on deep cover depths

Results are presented in Table 4.3. Note that in this table, section 40 with the section properties at crown governs.

Table 4.3: Structural adequacies for 3660 mm cover depth

Load combination	Short-term creep modulus		One week creep modulus	
	Middle axle at crown	Middle axle at shoulder	Middle axle at crown	Middle axle at shoulder
Deflection due to live load	11.94	9.76	9.02	7.33
Axial thrust only	1.13	1.12	1.04	1.01
Combined axial thrust and bending moment	1.21	1.21	1.08	1.07
Global buckling	10.19	9.64	12.84	12.29

4.2 Chamber's 50 Year Creep Modulus

4.2.1 Shallow cover depth

A sensitivity analysis was performed on the model with 610 mm cover depth to investigate the effects of 50 year creep modulus on the structural adequacies. A range of ± 30% of the given 50 year creep modulus was taken into consideration with an interval of 10%. Two loading cases were considered, being short-term live load and parking vehicle for one week duration. In each loading case, two locations of wheel loads were considered, e.g. wheel load at the crown and wheel load at the shoulder. The results are presented in Table 4.4, Table 4.5, and Figure 4.4. Adequacies of global buckling and deflection are not plotted because they have high safety margins.

Table 4.4: Structural adequacies vs. 50 year modulus under short-term live load for 610 mm cover depth

Changes in the initial E50 year (%)	-30	-20	-10	0	10	20	30
Calculated E 50 year value (MPa)	130.3	148.9	167.5	186.2	204.8	223.4	242.0
Deflection due to dead load (% of rise)	0.65	0.65	0.61	0.61	0.59	0.57	0.54
Thrust only due to wheel load at crown	2.52	2.57	2.66	2.70	2.76	2.82	2.88
Thrust only due to wheel load at shoulder	2.34	2.39	2.47	2.50	2.56	2.61	2.66
Combined thrust and bending moment due to wheel load at crown	3.25	3.33	3.47	3.53	3.63	3.71	3.82
Combined thrust and bending moment due to wheel load at shoulder	3.14	3.22	3.36	3.42	3.50	3.59	3.69
Global buckling due to wheel load at crown	6.02	6.23	6.45	6.63	6.81	6.97	7.14
Global buckling due to wheel load at shoulder	5.45	5.65	5.85	6.02	6.18	6.34	6.49

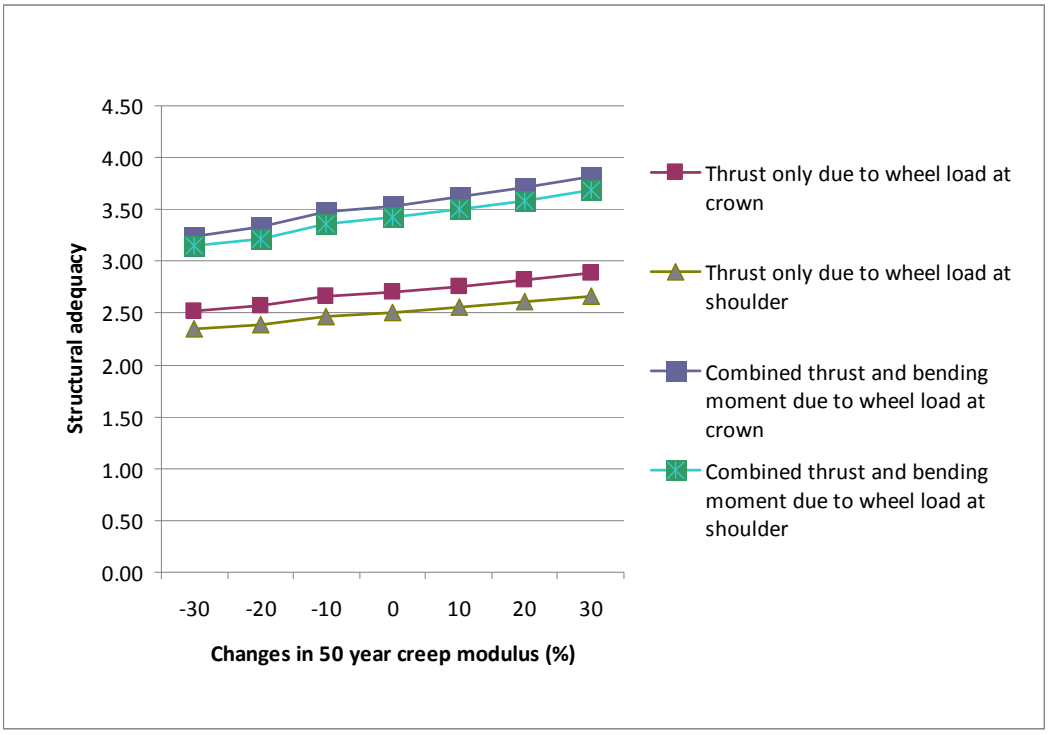

Figure 4.3: Structural adequacies vs. 50 year modulus under short-term live load for 610 mm cover depth

Table 4.5: Structural adequacies vs. 50 year modulus under one week live load for 610 mm cover depth

Changes in the initial E 50 year (%)	-30	-20	-10	0	10	20	30
Calculated E 50 year value (MPa)	130.3	148.9	167.5	186.2	204.8	223.4	242.0
Deflection due to dead load (% of rise)	0.65	0.65	0.61	0.61	0.59	0.57	0.54
Thrust only due to wheel load at crown	1.38	1.40	1.43	1.45	1.46	1.48	1.50
Thrust only due to wheel load at shoulder	1.29	1.31	1.33	1.34	1.36	1.38	1.39
Combined thrust and bending moment due to wheel load at crown	1.78	1.81	1.86	1.88	1.91	1.94	1.97
Combined thrust and bending moment due to wheel load at shoulder	1.74	1.76	1.81	1.83	1.86	1.89	1.92
Global buckling due to wheel load at crown	8.63	8.91	9.21	9.43	9.66	9.88	10.11
Global buckling due to wheel load at shoulder	8.12	8.38	8.67	8.88	9.10	9.31	9.53

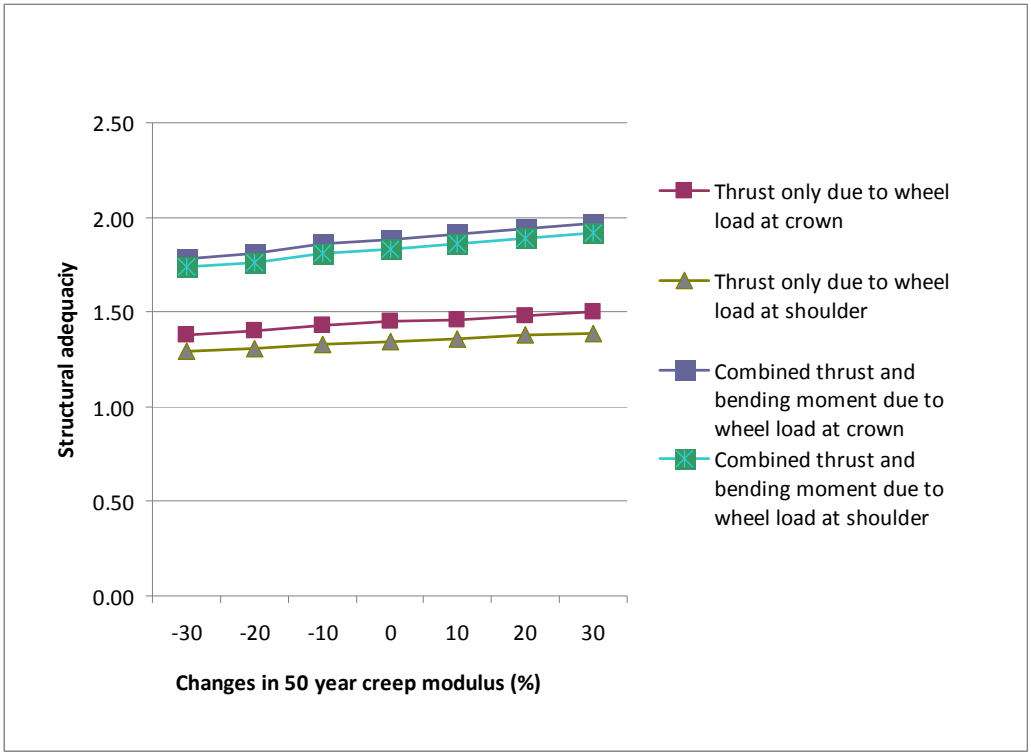

Figure 4.4: Structural adequacies vs. 50 year modulus under one week live load for 610 mm cover depth

It can be derived from the above tables and figures that the structural adequacies do not change significantly when the 50 year creep modulus varies. All structural adequacies change less than 11% when there is 30% variation in the 50 year modulus. This is due to the fact that the short-term

response to live load (short-term modulus) dominates the capacity calculation. The sensitivity of the 50 year creep value will have more impact on the maximum culvert depth.

4.2.2 Deep cover depth

Similar analyses were conducted for the cover depth of 3500 mm, however, only for the case of one week loading as this case is more critical than short-term loading. For this analysis case, the effects of dead load with long-term modulus are more significant than the effects of live load with short-term modulus, thus the A160 loading is used instead of M1600 loading for simplicity. Results are shown in Table 4.6 and displayed in Figure 4.5. Adequacies of global buckling and deflection are not plotted because they have high safety margins.

Table 4.6: Structural adequacies vs. 50 year modulus under one week live load for 3500 mm cover depth

Changes in the initial E 50 year (%)	-30	-20	-10	0	10	20	30
Calculated E 50 year value (MPa)	130.3	148.9	167.5	186.2	204.8	223.4	242.0
Deflection due to dead load	3.60	3.40	3.24	3.10	2.99	2.89	2.80
Thrust only due to wheel load at crown	0.91	0.99	1.07	1.15	1.22	1.30	1.37
Thrust only due to wheel load at shoulder	0.87	0.95	1.02	1.09	1.15	1.22	1.28
Combined thrust and bending moment due to wheel load at crown	0.91	1.02	1.12	1.22	1.33	1.43	1.53
Combined thrust and bending moment due to wheel load at shoulder	0.89	1.00	1.10	1.20	1.30	1.40	1.50
Global buckling due to wheel load at crown	12.42	12.44	12.49	12.54	12.59	12.65	12.72
Global buckling due to wheel load at shoulder	11.29	11.35	11.43	11.50	11.58	11.66	11.74

It should be noted that the study undertaken to investigate the sensitivity of the effect of young's modulus on the maximum culvert depth is based on the assumption that the limiting strain remains the same for the different young's modulus values. Whether this is achievable in reality is dependent on many factors. The limiting strain is typically related to the resin used rather than other factors as stated in ASTM F2787-09 and is determined by testing by the manufacturer. As this is a theoretical study no such information is available so the constant limiting strain assumption is considered the only reasonable basis for the comparison. If actual changes in the young's modulus of the product were contemplated, testing would be required to confirm the performance of the material and the 3.3% limiting strain assumption. The results from the following analysis shall be used in consideration of the assumptions and limitation above.

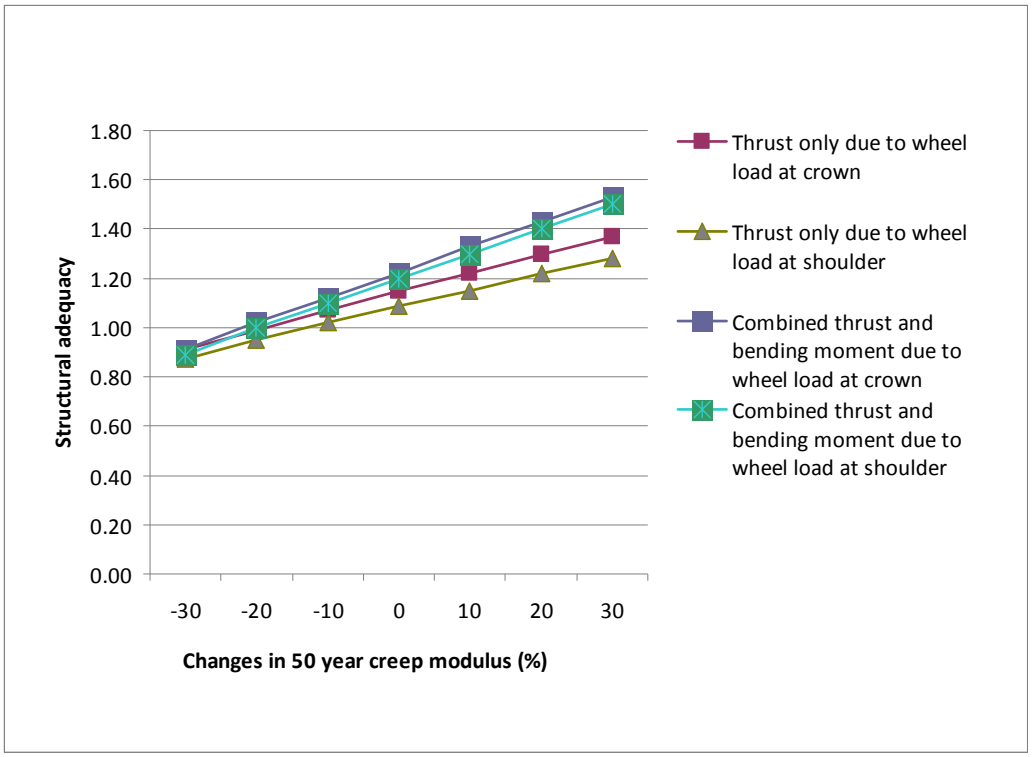

Figure 4.5: Sensitivity of structural adequacies under one week live load

As expected for deep cover cases, the structural adequacies are more dependent on the 50 year creep modulus due to the high dead load component. While the global buckling adequacies are almost unchanged, changes in structural adequacies in thrust and combined thrust and bending capacities are of the same magnitude as the changes in the 50 year creep modulus.

5 CONCLUSIONS AND RECOMMENDATIONS

- The calculated minimum cover depth is 470 mm. The critical actions occur under the W80 load, being deflection and axial thrust due to one week live load. A 600 mm cover depth matches well with the requirement of minimum cover of 600 m for pipes subject to vehicle loading in AS/NZS 2566:1998 (Clause 3.2.5). This number is also recommended by McGrath (2010) in a recent structural evaluation of the DC-780 chamber under AASHTO LRFD loadings for unpaved situations where rutting might reduce the depth of the fill over time.
- The calculated maximum cover depth of 3660 mm was found to be safe for the chamber. The critical action occurs under the M1600 load, being axial thrust due to one week live load.
- For shallow cover configurations, the structural capacity of the chamber has limited sensitivity to the 50 year creep modulus.
- For deep cover configurations, the structural adequacies vary more significantly when the 50 year creep modulus changes. The structural adequacy factor generally changes in proportion to the change in the 50 year modulus.
- If the minimum depth of foundation is adopted as per the StormTech manual at 230 mm, the subgrade required allowable bearing capacity needs to be 250 kPa.

REFERENCES

AASHTO 2010, AASHTO LRFD Bridge Design Specifications, Interim 2010 Version

AS 5100 2004, *Bridge Design Standard*, Australian Standard, Standards Australia, Sydney, Australia.

AS/NZS 2041 1998, *Buried Corrugated Metal Structures*, Australian/New Zealand Standard, Standards Australia and Standards New Zealand.

AS/NZS 2041.1 forthcoming, 'Buried corrugated metal structures: part 1: design methods', draft no. DR 10015 CP (2010).

AS/NZS 2566 1998, *Buried Flexible Pipelines*, Australian/New Zealand Standard, Standards Australia and Standards New Zealand.

ASTM F2787-09, *Standard Practice for Structural Design of Thermoplastic Corrugated Wall Stormwater Collection Chambers*, ASTM International, Pennsylvania, United States.

ASTM F2418-09, S*tandard Specification for Polypropylene Corrugated Wall Stormwater Collection Chambers,* ASTM International, Pennsylvania, United States.

Katona MG, Mlynarski M, and McGrath TJ 2008, '*CANDE-2007 Culvert Analysis and Design – Solution Methods and Formulations*', TRB NCHRP 619, Transportation Research Board, Washington, United States.

Mlynarski M, Katona MG and McGrath TJ 2008, '*CANDE-2007 Culvert Analysis and Design – User Manual and Guideline*', TRB NCHRP 619, Transportation Research Board, Washington DC, United States.

StormTech 2006, StormTech Design Manual, StormTech LLC, Connecticut, USA.